Z. Arb. Wiss. (2023) :126–144
https://doi.org/10.1007/s41449-022-00341-7

WISSENSCHAFTLICHE BEITRÄGE

Towards intelligent illumination systems: from the basics of light science to its application

Babak Zandi[1] · **Tran Quoc Khanh**[1]

Accepted: 8 June 2022 / Published online: 2 December 2022

Abstract

The development and design of lighting systems is closely linked to the physiology of the human visual system. Whereas with the first generation of light sources, the visual appearance of objects in an illuminated environment was only possible by adjusting the level of illuminance. In contrast, with modern semiconductor light-emitting diode (LED) systems, the emitted spectrum can be flexibly varied. This new degree of freedom has led to an interdisciplinary field of research, aiming to explore the effect of light on humans in terms of physiological, psychological and cognitive parameters and to model their mechanisms or make them quantifiable via mathematical metrics. Today's quality assessment of light spectra is composed of metrics that combine colour perception, contrast sensitivity, visual sensation, non-visual responses and cognitive preference. A lighting system that takes these aspects into account is commonly referred to as an integrative lighting solution or Human Centric Lighting. This article describes the current knowledge about the human eye's visual and non-visual processing system, the development of colour rendering metrics, and the light-induced effect on nocturnal melatonin suppression. Then, the basic concept of an intelligent and individually adaptable lighting system will be discussed. *Practical Relevance:* This article deals with the basics of light science and covers the fundamental aspects of intelligent lighting systems, which with the help of multi-channel LED luminaires, could address the visual properties of light and the human circadian system separately via metameric spectra.

Keywords Integrative lighting technology · Human Centric Lighting · Visual performance · Non-image forming lighting effects.

✉ Dr.-Ing. Babak Zandi
zandi@lichttechnik.tu-darmstadt.de

Prof. Dr.-Ing. habil. Tran Quoc Khanh
khanh@lichttechnik.tu-darmstadt.de

[1] Fachbereich Elektro- und Informationstechnik, Fachgebiet für Adaptive Lichttechnische Systeme und Visuelle Verarbeitung, Technische Universität Darmstadt, Hochschulstraße 4a, 64289 Darmstadt, Germany

Auf dem Weg zu intelligenten Beleuchtungssystemen: von den Grundlagen der Lichtwissenschaften zu ihrer Anwendung

Zusammenfassung

Die Entwicklung und Auslegung von lichttechnischen Systemen ist eng an die Physiologie des menschlichen Sehsystems gekoppelt. Während mit der ersten Generation von Lichtquellen, die visuelle Erscheinung von Objekten in einer beleuchteten Umgebung durch die Höhe der Beleuchtungsstärke beeinflusst wurde, kann mit modernen Halbleiter-LED Systemen ein Lichtspektrum flexibel angepasst werden. Dieser neue Freiheitsgrad hat zu einem interdisziplinären Forschungsfeld geführt, welches sich zum Ziel gesetzt hat, die Wirkung von Licht auf den Menschen hinsichtlich physiologischer, psychologischer und kognitiver Parameter zu erforschen und deren Wirkmechanismen zu modellieren oder mit Metriken quantifizierbar zu machen. Die heutige Qualitätsbewertung von Lichtspektren setzt sich aus Messgrößen zusammen, die Farbwahrnehmung, Kontrastempfindlichkeit, visuelle Empfindung, nicht-visuelle Modulation und kognitive Präferenz miteinander vereint. Ein lichttechnisches System, welches diese Aspekte berücksichtigt, wird gemeinhin als integrative Beleuchtungslösung oder Human Centric Lighting bezeichnet. Der vorliegende Beitrag beschreibt übersichtlich die modernen Kenntnisse des visuellen und nicht-visuellen Verarbeitungssystems, die Entwicklung der Farbwiedergabe und der Lichtwirkung auf die Melatonin-Suppression. Anschließend wird das Grundkonzept eines intelligenten und individuell anpassbaren Beleuchtungssystems diskutiert.

Praktische Relevanz: Der Beitrag behandelt die Grundlagen der Lichttechnik und geht anschließend auf das Grundkonzept von intelligenten Beleuchtungssystemen ein, welche mittels Mehrkanal LED-Leuchten zukünftig in der Lage sein werden, die visuellen Eigenschaften des Lichtes und das menschliche zirkadiane System durch metamere Spektren getrennt voneinander anzusprechen.

Schlüsselwörter Integrative Lichttechnik · Human Centric Lighting · Visuelle Leistung · Nicht-visuelle Lichtwirkung.

1 Introduction

The science of lighting technology originally worked on developing appropriate light sources and applying them in indoor lighting systems to support the humans' visual perception when natural daylight harvesting is limited or unfeasible. One conventional goal of artificial light is to optimize the visual performance in terms of visual acuity, which can be affected by varying the irradiance in the indoor environment (Cavonius and Robbins 1973). When performing visual tasks under dim lighting conditions that require sharp vision, the visual system could be stressed as the eye's lens accommodation is less effective in maintaining the image distance at the level of the fovea centralis in the retina (Johnson 1976). Generally, an increased illuminance is preferable to enable sharp vision. However, adjusting the illumination too bright the visual acuity and contrast sensitivity, i.e. visual performance, could be reduced due to glare (Sturgis and Osgood 1982; Hamedani et al. 2020b), which additionally could cause a discomfort working environment for visual tasks (Osterhaus 2005; Geerdinck et al. 2014; Hamedani et al. 2019, 2020a). In other words, the optimal illuminance level in interior lighting is from a physiological point of view is within a specific range, whose identification requires knowledge of how the eye's visual system processes and perceive light. Therefore, the development of lighting metrics that can quantify the human's visual sensation in response to light spectra regarding brightness, colour and contrast perception, including visual comfort, is an essential aspect for evaluating the quality of light (DiLaura 2009; Van Den Wymelenberg and Inanici 2014; Boyce and Smet 2014; Kruisselbrink et al. 2018; Bodrogi et al. 2019).

A major change in light science research was initiated after a new type of photoreceptors in the outer retina was discovered, namely the intrinsically photosensitive ganglion cells (ipRGCs), which can affect the human's non-visual responses such as nocturnal melatonin suppression, steady-state pupil light reflex or even cognitive performance measures (Provencio et al. 1998, 2000; Gooley et al. 2001, 2003; Berson et al. 2002; Hattar et al. 2002; Tu et al. 2005). The ipRGCs express the photopigment melanopsin and exhibit a peak wavelength-sensitivity around 480 nm (Lucas et al. 2014, 2020; CIE 2018a; Spitschan 2019). Consequently, a light spectrum needs to have enough spectral power in the short-wavelength range during the morning hours to be biologically effective concerning non-visual responses. In contrast, before bedtime, the spectral power in the short-wavelength range needs to be low to prevent melatonin suppression and support the human's circadian rhythm (Stefani et al. 2021; Stefani and Cajochen 2021; Shishegar et al. 2021; Zandi et al. 2021c). Therefore, the today's research of artificial indoor illumination faces the challenge of balancing the goals of satisfying legal requirements, minimizing the energy consumption while enhancing the human's visual performance, visual preference and considering the biological impact of light (Zandi et al. 2021a).

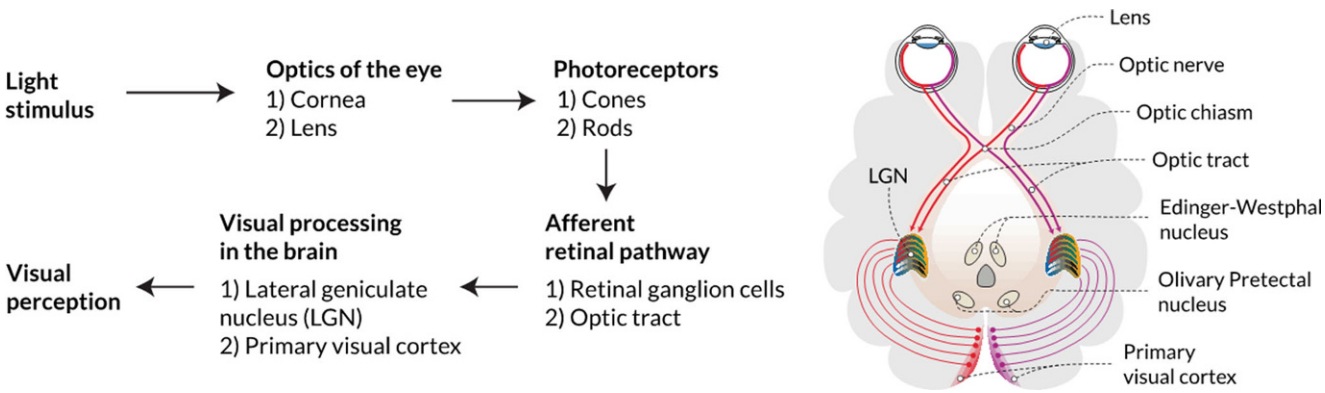

Fig. 1 Simplified processing pathway of the human's visual perception in response to light. (The Figure is reprinted from Zandi 2022 under CC BY-SA 4.0 license)

Abb. 1 Vereinfachte Verarbeitungskette der visuellen Wahrnehmung des Menschen in Reaktion auf Lichtreize. (Die Abbildung stammt aus der Arbeit von Zandi 2022, übernommen mit einer CC BY-SA 4.0 Lizenz)

In this work, the basics of the eye's physiology, light science and the essential lighting-related metrics widely applied to assess light's impact on visual and non-visual responses will be discussed. Next, the concepts of smart lighting systems will be introduced. Followed by a discussion of their drawback in the possibility of acknowledging both visual preference and non-visual biological necessity at the same time. Finally, the technique of applying metameric light (Allen et al. 2018; Souman et al. 2018; Zandi et al. 2021a, c) is discussed, which allows to tune the human's non-visual responses without altering the visual properties of an illumination. This approach may become part of the next generation of intelligent lighting systems as it is a technique that can balance a human's visual preference with the non-visual properties of light. Note that the text provided in section two and three is reprinted from B.Z.'s doctoral thesis (Zandi 2022).

2 Quantifying the visual properties of artificial light

The optical system of the eye projects visual stimuli onto the retina, which let the photoreceptors in the outer retinal segment respond with graded membrane potential changes. A stack of interconnected retinal cell layers further processes and transmits these electrical signals to the ganglion cells that relay frequency-encoded action potentials to retinorecipient neurons in the brain. The visual processing of the human's visual sensation steps can be divided into four parts: (i) the optical apparatus of the eye that focuses visual stimuli on the retina; (ii) the photoreceptors, which absorb light quanta and convert them into electrical signals by a phototransduction mechanism; (iii) the downstream retinal processing layers that encode spatial stimuli for the brain; (iv) the distribution and processing of the transformed visual stimuli inside the brain for visual perception (Fig. 1).

The outer retina of the human eye is spatially clustered with photoreceptors that are classified into cones and rods, responsible for absorbing the light quanta that pass the eye's ocular system. Transforming the light quanta into graded membrane potentials, takes place in the outer segment of the retinal photoreceptors in which the light-sensitive photopigments (opsin) are located inside several stacked layers of so-called discs (Valberg 2005, chapter 3). Rods are shaped for low light conditions as they contain a higher concentration of photopigments, arranged in layered discs with longer axial length, resulting in a greater possibility of capturing individual photons (Valberg 2005, chapter 3). As a result, rods can even respond to a single photon due to their high amplification (Tinsley et al. 2016). The photopigment concentration and the number of layered discs in the outer receptor's segments are lower in cones. Therefore, they require more light quanta for triggering a comparable cell membrane response (Valberg 2005, chapter 3). The photoreceptors, however, can be classified according to their spectral absorption sensitivity, respective peak response λ_{Peak}, integration time, temporal resolution in the retina and the responding range at different (ir)radiance levels. In photopic lighting conditions (i.e., during the day), the cones are responsible for driving the human's colour and brightness sensation. The human retina has three types of cones with partly overlapping spectral absorption sensitivities, but distinct peak-responses with (i) the short-wavelength-sensitive cones that contain an opsin called cyanolabe (S-cones, $\lambda_{Peak} \approx 420\,nm$), (ii) the medium-wavelength-sensitive cones that contain the opsin chlorolabe (M-cones, $\lambda_{Peak} \approx 535\,nm$), and (iii) the long-wavelength-sensitive cones that contain the opsin erythrolabe (L-cones, $\lambda_{Peak} \approx 565\,nm$) (Stockman and Sharpe 2000; Solomon and Lennie 2007; Lucas et al. 2014; Zandi et al. 2021b). Rods contain the photopigment rhodopsin

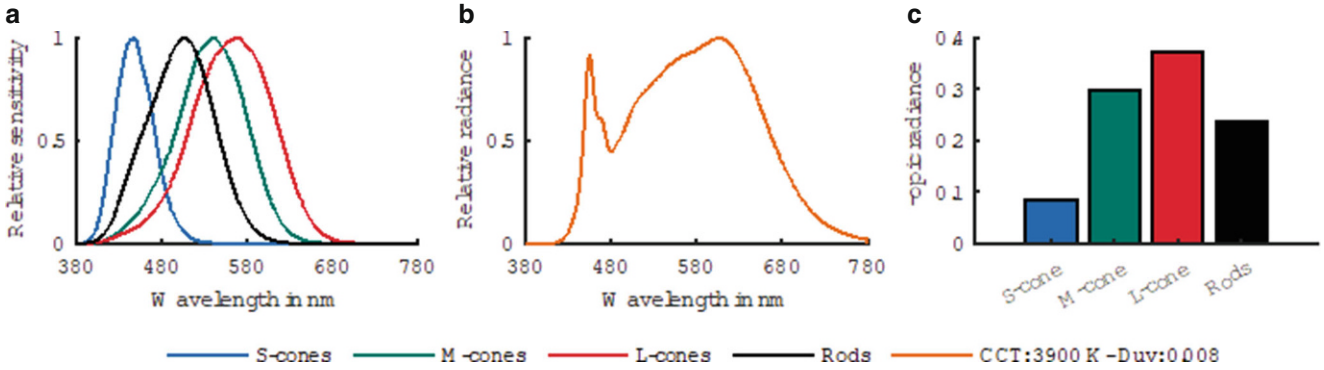

Fig. 2 Steps of computing the α-opic radiance values by using the action spectra of the cones and rods as specified in the CIE S026/E:2018. **a** Photoreceptor sensitivity, **b** Sample spectrum, **c** α-opic values

Abb. 2 Schritte zur Berechnung der α-opischen Strahldichtewerte unter Verwendung der Wirkungsspektren der Zapfen und Stäbchen gemäß der CIE S026/E:2018. **a** Empfindlichkeitskurven der Photorezeptoren α, **b** Beispielspektrum, **c** α-opischen Werte

(Lucas et al. 2014), exhibiting a peak response λ_{Peak} at approximately 500 nm. However, the inter-observer's spectral sensitivities may differ due to the pre-receptoral filtering by the crystalline lens and dens of macular pigmentation in the fovea, which is also a function of age (Gegenfurtner and Sharpe 1999, chapter 2). For example, when considering the pre-receptoral filtering for a standard observer, the peak sensitivity of the rods is altered to 507 nm, 448 nm for the S-cones, 542 nm, for the M-cones and 570 nm for the L-cones (Lucas et al. 2014; CIE 2018a).

In 2018, the International Commission on Illumination (CIE) introduced the α-opic system (CIE S026/E:2018) to standardize the photoreceptors' sensitivity functions using the 10°-cone fundamentals from Stockman & Sharpe (Stockman and Sharpe 2000) and the rod sensitivity with the V'(λ) function for scotopic vision, ensuring better comparability between research results (CIE 2018a) (see Fig. 2a). According to the CIE standard, the photoreceptor's action spectra should be written as $s_{\alpha}(\lambda)$ with the α-opic prefix α that denotes one of the opsin-based photopigments, namely $s_{\text{sc}}(\lambda)$ for S-cones, $s_{\text{mc}}(\lambda)$ for the M-cones, $s_{\text{lc}}(\lambda)$ for L-cones and $s_{\text{rh}}(\lambda)$ for the absorption sensitivity of the rods (CIE 2018a).

These action spectra are used in fundamental aspects of light science to quantify the impact of distinct light spectra on the human photoreceptor response. For this, the photobiological α-opic radiance, for example, can be calculated with

$$L_{e,\alpha} = \int_{380\,\text{nm}}^{780\,\text{nm}} L_e(\lambda) \cdot s_{\alpha}(\lambda)\, d\lambda \tag{1}$$

where $L_e(\lambda)$ is defined as the spectral radiance and $s_{\alpha}(\lambda)$ denotes the respective action spectrum of a photoreceptor's opsin. Note that the Eq. 1 can also be used to compute the α-opic irradiance by replacing $L_e(\lambda)$ with the spectral irradiance $E_e(\lambda)$ of a light stimulus. In Fig. 2b, a phosphor converted light-emitting diode (LED) spectrum is leveraged (luminance = 230.33 cd/m^2) to compute its α-opic radiance values (see Fig. 2c). Spectra can be characterised by its chromaticity coordinate or the correlated colour temperature (CCT) if the chromaticity coordinate is placed near the Planckian locus. When specifying a spectrum using a CCT value, the distance to the Planckian locus must also be reported with the Duv value (see Sect. 2.3), which is specified in the CIEuv-1960 colour space. For example, the reported sample spectrum in Fig. 1b yields a CCT of 3900 K with a Duv distance to the Planckian locus of 0.008.

2.1 Cone opponency and projections to the brain

The photoreceptors' action spectra (Fig. 2a) describe the probability of catching, absorbing and transforming light quanta with a distinct wavelength into a graded membrane potential (Solomon and Lennie 2007). Consequently, individual photoreceptors are colour blind (Dacey 2000; Solomon and Lennie 2007; Conway et al. 2010; Spitschan and Woelders 2018), as no spectral information can be derived from an electrical signal at the cell's dendrites after photon catch. Colour perception originates from the comparison between the signals of different retinal cone types (Field et al. 2010). This effect is called the principle of univariance (Solomon and Lennie 2007; Spitschan and Woelders 2018), stating that two light stimuli with different spectral power distributions can trigger the same visual sensation if the α-opic values across the cones are identical. Colour information features are encoded in the retina with cone-opponency circuits, through which cone signals are compared by either lateral processing in the outer plexiform layer (centre surround antagonistic) or through the retinal ganglion cells (RGCs) that stratify and synapse with different types of ON-/OFF bipolar cells in the inner plexiform layer (Conway et al. 2018).

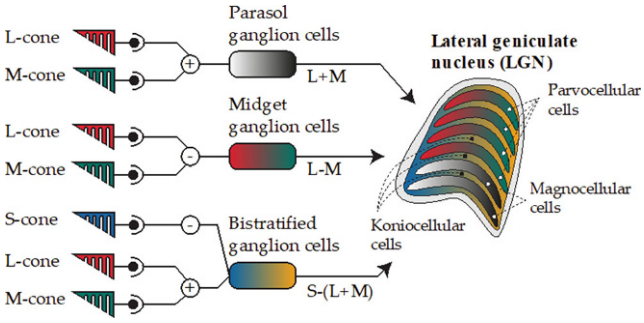

Fig. 3 Visual processing in der lateral geniculate nucleus (LGN). (The Figure is reprinted from Zandi 2022 under CC BY-SA 4.0 license)
Abb. 3 Visueller Verarbeitungspfad von der menschlichen Netzhaut bis zum visuellen Kortex. (Die Abbildung stammt aus der Arbeit von Zandi 2022, übernommen mit einer CC BY-SA 4.0 Lizenz)

According to Field et al. (Field et al. 2010), three types of ganglion cells, namely, the parasol midget and small bistratified ganglion cells account for about 75% of all RGCs, responsible for transmitting frequency-coded action potentials to retinorecipient brain nuclei (Solomon and Lennie 2007; Smith et al. 2008) (see Fig. 3). The ganglion cells' axons project to the lateral geniculate nucleus (LGN) of the thalamus, the relay station (Solomon and Lennie 2007), i.e. gateway to the brain's primary visual cortex V1 that processes that visual sensory information further (see Fig. 1). Morphologically, the LGN is structured into six different layers, of which the lowest two pieces consist of magnocellular (M) cells and the upper four of the parvocellular (P) cells (Martinovic 2015). In between the M- and P-cells of the LGN, six additional layers are located containing koniocellular (K) cells (Martinovic 2015). Each layer type of the LGN conveys encoded colour and brightness properties of visual stimuli via the parvocellular (PC), magnocellular (MC) and koniocellular (KC) pathways (Smith et al. 2008) to the primary visual cortex (see Fig. 1). P- and K-cells in the LGN show strong opposing colour responses, while the M-cells are mostly sensitive to luminance information (Gegenfurtner 2003). The cone-opponency is often compared using the early psychophysical theory of (Hering 1920), who postulated that colour perception is created by a system of separate antagonistic channels with the complementary colours red-green, yellow-blue, and one luminance, i.e. brightness channel consisting of achromatic black-white information (Kingdom and Mullen 1995). When mapping the psychophysical colour-opponency theory into the physiological architecture of cone-opponency, a similar mechanism can be found at the level of the LGN. Midget ganglion cells provide cone opponent colour information to the PC-pathway, derived from a subtraction of L- and M-cones (L − M, red-green opponency), showing significant responses to chromatic modulation (Lee 2004; Solomon and Lennie 2007; Smith et al. 2008; Wool et al. 2019). Bistratified ganglion cells target the middle KC-layers and provide excitatory signals from S-cones with opposed inhibitory information from an additive L- and M-cones signal combination (S − (L + M), blue-yellow opponency) (Tailby et al. 2008; Martinovic 2015; Wool et al. 2019). Parasol ganglion cells project to the magnocellular layers of the LGN, providing an achromatic luminance signal from L- and M-cones (L + M, brightness) (Jennings and Martinovic 2014). Note that the perceptual colour-opponency originally proposed by Ewald Hering differs from the cone-opponency mechanism at the level of the LGN, meaning the nomenclature of the channels with a hue association, i.e. red-green, has historical reasons but is incorrect from a physiological perspective (Conway et al. 2018), as reviewed by (Shevell and Martin 2017).

Apart from the visual processing chain behind colour perception (Fig. 1), the brightness sensation's quantification is essential in photometry since radiant quantities are not perceived uniformly across the visible spectrum range due to the human eye's quantal catch probability and cone-opponency mechanism. Although the achromatic luminance channel (MC-pathway) seems to be separated from the opponent channels (KC- and PC-pathway) at the level of the LGN (Fig. 3), visual experiments reveal cone-opponency influences (Tsujimura et al. 2007; Ripamonti et al. 2009; Conway et al. 2018). The interaction of the achromatic luminance (L + M) and two opponent colour channels (L − M, S − (L + M)) (Sagawa 2006; Jennings and Martinovic 2014) lead to the fact that humans do not necessarily perceive a different set of light spectra at steady radiance $L_e(\lambda)$ as equally bright. Therefore, the discussed physiological and psychophysical visual response in this section become of practical interest, for example, in the methodological development of the luminous efficiency function (Sharpe et al. 2005), the fundamental basis of photometry and light science.

2.2 The chromaticity of a light source

The shape of a spectral power distribution (SPD) is a minor criterium outside the discipline of spectral matching or daylight simulation. Lighting metrics computed from an SPD are more of value as they can be used to describe the spectrum's impact on the human's visual pathway or the photoreceptor's responsiveness level. However, mostly lighting metrics aim to specify the human's perception regarding chromaticity, colour quality or visual preference for a light source in an illuminated environment. The previously discussed sensitivity functions of the cones are rather on a physiological level while so-called lighting metrics account for the whole process from the physiological processing of light quanta up to the psychophysical perception of light.

In 1931, the CIE proposed the colour matching functions (CMFs) $\overline{x}(\lambda)$, $\overline{y}(\lambda)$ and $\overline{z}(\lambda)$ based on the experimental results of W.D. Wright (Wright 1929) and J. Guild (Guild 1931) to quantify the human colour sensation in response to a light spectrum (Schanda 2007, chapter 3) for a viewing angle of 2°. The CMFs can be used to map the human colour perception of a trichromatic observer in the CIExy-1931 colour space (CIE 2004). Firstly, the tristimulus values *X, Y* and *Z* need to be computed from the light spectrum $S(\lambda)$ with

$$\begin{aligned} X &= K\int_{380\,\mathrm{nm}}^{780\,\mathrm{nm}} \overline{x}(\lambda)\cdot S(\lambda)\,d\lambda, \\ Y &= K\int_{380\,\mathrm{nm}}^{780\,\mathrm{nm}} \overline{y}(\lambda)\cdot S(\lambda)\,d\lambda \quad \text{and} \\ Z &= K\int_{380\,\mathrm{nm}}^{780\,\mathrm{nm}} \overline{z}(\lambda)\cdot S(\lambda)\,d\lambda. \end{aligned} \tag{2}$$

For self-luminous objects where $S(\lambda)$ is measured in a radiometric unit, the constant K should be set to the luminous efficiency of radiation value $K_m = 683\,\mathrm{lm/W}$. The colour matching function $\overline{y}(\lambda)$ is equal to the luminous efficiency function $V(\lambda)$ for photopic vision (Schanda 2007, chapter 3). Hence the tristimulus value Y is proportional to the photometrics counterpart of $S(\lambda)$ when using $K = K_m$ (Schanda 2007, chapter 3). In colorimetry, however, the constant K is irrelevant when calculating the chromaticity coordinates *x, y* and *z* of the CIExy-1931 colour space (see Eq. 3), as

$$\begin{aligned} x &= \frac{X}{X+Y+Z}, y = \frac{Y}{X+Y+Z}, \\ z &= \frac{Z}{X+Y+Z} = 1-x-y \end{aligned} \tag{3}$$

It is sufficient to report only the (*x, y*) values, since $x + y + z = 1$ (Schanda 2007; Babilon 2018). The underlying experiments for the trichromatic system of the CIExy-1931 colour space were done using a foveal visual field of 2°. Therefore, the 2°-CMFs may not be appropriate to describe colour sensation for visual fields larger than 4° (Schanda 2007) as a greater contribution of S-cones comes into play (Stockman et al. 1999). In 1964, the CMFs $\overline{x}_{10°}(\lambda)$, $\overline{y}_{10°}(\lambda)$ and $\overline{z}_{10°}(\lambda)$ were introduced for a 10° standard observer by the CIE, with which the chromaticity coordinates of the CIExy-1964 colour space can be calculated using Eq. 2 and 3.

Due to the larger visual field used in the colour matching experiments, the colour sensation in an illuminated environment is approximated better. Thus, in visual experiments with a visual field larger than 4°, it is recommended to apply the 10°-CMFs to compute the tristimulus values. However, the 2°-CMFs and hence the CIExy-1931 colour space are commonly used in the literature where only the specification of an SPD's chromaticity is of interest. Individual observers may have distinct colour sensations, although a fixed polychromatic light spectrum from a multi-channel LED luminaire is presented. This effect is denoted as observer metamerism (Eissfeldt et al. 2021). One reason is that the human's foveal L:M cone ratio (Rushton and Baker 1964; Kremers et al. 2000; Otake and Cicerone 2000; Carroll et al. 2002; Hofer 2005) can vary between individuals. Secondly, the human's lens and macular transmission are subject to individual variations, affecting the colour sensation (Hu et al. 2020). In other words, the individual CMFs of a human observer could deviate from the CIE standard observer (Eissfeldt et al. 2021).

However, an essential question in colour research is how large the distance between two chromaticity points can be so that an observer can perceive a just noticeable difference (JND) in chromaticity. A significant disadvantage of using the CIExy system is that the Euclidian distances between a reference point (x_c, y_c) and a second chromaticity coordinate (x, y) at which a JND occurs are not uniformly distributed in the colour space (Schanda 2007). Hence, no uniform threshold can be defined for the Euclidian distance

$$\Delta xy = \sqrt{(x-x_c)^2 + (y-y_c)^2} \tag{4}$$

between the CIExy-1931 chromaticity coordinate (x, y) and a reference (x_c, y_c) for preventing a noticeable difference in colour sensation. In 1942, David MacAdam found that the regions in the CIExy colour space where the chromaticities cannot be distinguished have the shape of an ellipse, which vary in size and orientation depending on the position of (x_c, y_c) (MacAdam 1942; Schanda 2007). The regions where no colour difference is visible are denoted as McAdam ellipses. In spectral optimization, tolerance values need to be set to define how far the chromaticity coordinate (x, y) of an optimized spectrum can differ from the target chromaticity point (x_c,y_c). Usually, one wants to select the tolerance so that no colour difference is visible between the selected target chromaticity point and the optimized one.

In order to retrieve a colour space in which the information is provided whether two chromaticity coordinates can be visually distinguished from each other (MacAdam 1937), the CIE uniform chromaticity scale diagram CIEu'v'-1976 was introduced (Schanda 2007). The McAdam ellipses can be reduced to circles in the CIEu'v'-1976 colour space and are perceptually more uniform (Schanda 2007) for white light sources with chromaticity coordinates placed near the Planckian locus (Yoshi and Blattner 2014). To project CIExy chromaticity coordinates into the CIEu'v'-1976 colour space, the transformations in Eq. 5 can be used (CIE 2004; Schanda 2007).

$$\begin{aligned} u' &= \frac{4X}{X+15Y+3Z} = \frac{4x}{-2x+12y+3} \\ v' &= \frac{9Y}{X+15Y+3Z} = \frac{9y}{-2x+12y+3} \end{aligned} \tag{5}$$

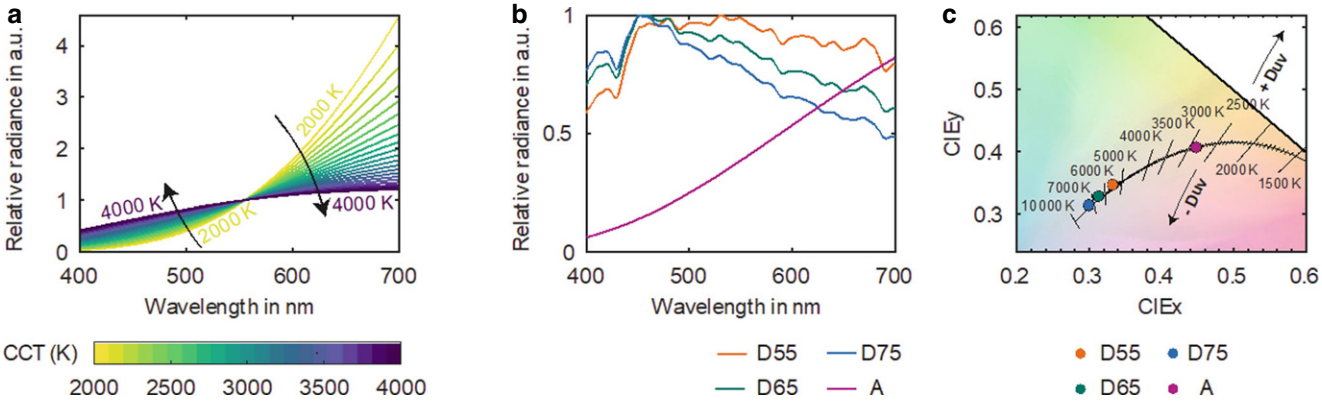

Fig. 4 Association between the spectra of the black body radiator and standard illuminants (D55, D65, D75 and A) with the Planckian locus in the CIExy-2° colour space. (The Figure is reprinted from Zandi 2022 under CC BY-SA 4.0 license)

Abb. 4 Zusammenhang zwischen den Spektren eines Schwarzkörperstrahlers im sichtbaren Spektralbereich und der Normlichtquellen (D55, D65, D75 und A) mit dem Planckschen Kurvenzug im CIExy-2° Farbraum. (Die Abbildung stammt aus der Arbeit von Zandi 2022, übernommen mit einer CC BY-SA 4.0 Lizenz)

According to the CIE TN 001:2014, for the JND regions in the CIEu'v'-1976 colour space, the definition of the *n*-step MacAdam circle should be applied. The radius of a *n*-step MacAdam circle can be computed with $n \cdot 0.0011$ (Yoshi and Blattner 2014). When the Euclidean distance between two CIEu'v'-1976 chromaticity points is $\Delta u'\ v' = 0.0011 \cdot 1.18 \approx 0.0013$, the probability that observers detect a chromaticity difference is at 50% (Yoshi and Blattner 2014). Thus, if the chromaticity coordinate of an optimized spectrum lies within one McAdam step, where the target chromaticity point (x_c, y_c) is the centre, an observer may not perceive a colour difference as $\Delta u'v' = 0.0011$ is below the absolute threshold.

2.3 Using the correlated colour temperature as proxy for chromaticity

Although the human's colour sensation in response to a spectral power distribution can be identified using the CIExy-1931 or CIEu'v'-1976 colour space, it is familiar to report the chromaticity of white light sources using a correlated colour temperature (CCT). The definition of colour temperature is coupled to the emitted spectra of a Planckian (black body) radiator. According to the CIE 015:2018 (Annex E) (CIE 2018b), the spectrum of the black body radiator can be calculated using the formula

$$L_{e,\lambda}(\lambda, T) = \frac{c_1 \cdot \lambda^{-5}}{\pi}\left[\exp\left(\frac{c_2}{\lambda \cdot T}\right) - 1\right]^{-1} \quad (6)$$

where $c_1 = 2\pi hc^2$ and $c_2 = hc/k$ with h as Planck's constant, c as speed of light in vacuum and k as Boltzmann constant. For colorimetric applications, the constant c_1 can be neglected since, only the relative SPD is of interest. The chromaticity coordinates of the SPDs (Fig. 4a) can be computed and plotted into CIExy-1931 colour space. The result is a curve denoted as the Planckian locus, with which CIExy-1931 chromaticity coordinates can be linked to a colour temperature. For example, if the chromaticity point of a test light source is placed directly on the locus, it is handier to report the associated colour temperature instead of the (x, y) coordinates. For illustration, the standard illuminants D55, D65, D75 and A were used (Fig. 4b) as test light sources and their chromaticity coordinate was plotted into the CIExy-1931 colour space (Fig. 4c), showing how the chromaticities are linked to the CCT values of the black body radiator.

The term correlated colour temperature (CCT) should be used for chromaticity coordinates, placed above or below the locus. Since the chromaticity points lie outside of the locus, the CCT is calculated using the Judd lines, which are orthogonal to the Planckian locus in the CIEuv-1960 colour space (Kelly 1963; Schanda and Danyi 1977). The associated CCT of a chromaticity coordinate is then defined by the intersection of the corresponding Judd line with the Planckian locus. Therefore, the CCT can also be used to define the chromaticity of white light sources if additional information regarding the orthogonal distance (Duv) to the Planckian locus is provided. If the chromaticity coordinate is below the locus, the Duv value becomes negative. As reported by (Durmus 2021), the distance of a test light source's chromaticity coordinate (u′, v′) to the Planckian locus (u_T', v_T') can maximally be

$$\Delta u'v' = \sqrt{\left(u_T' - u'\right)^2 + \frac{4}{9} \cdot \left(v_T' - v'\right)^2} = 0.05 \quad (7)$$

Otherwise, the association to a CCT value is not valid. To calculate the CCT from a chromaticity coordinate of a test light source, different formulas have been proposed in the literature for approximation (Robertson 1968; Schanda

et al. 1978; Krystek 1985; Xingzhong 1987; McCamy 1992; Hernández-Andrés et al. 1999; Ohno 2014; Li et al. 2016; Zhang 2019). For example, C. McCamy (McCamy 1992) proposed the third-order polynomial equation

$$\begin{aligned} \mathrm{CCT}_{\mathrm{Approx}} &= -449\mathrm{K}\cdot n^3 + 3525\mathrm{K}\cdot n^2 \\ &\quad - 6823.3\mathrm{K}\cdot n + 5520.33\mathrm{K} \end{aligned} \tag{8}$$

where n is defined as $(x–0.3320)/(y–0.1858)$ and (x, y) are the chromaticity points of the light source from which the CCT needs to be computed. The approximation error of Eq. 8 is between –4.25 K and 3.4 K for the CCT range $2105\,\mathrm{K} \le \mathrm{T} \le 8000\,\mathrm{K}$ (McCamy 1992). For CCTs greater than 10,000 K, the formula should be avoided as the estimation error at 12,500 K, for example, is 388 K (McCamy 1992). The formula of Y. Ohno (Ohno 2014) or the iterative approach by Li et al. (Li et al. 2016) can be used for more accurate calculations. However, the method by Li et al. (Li et al. 2016) is recommended, which provides with a tolerance of 10^{-3} K a reliable approximation of the CCT (Durmus 2021).

2.4 The colour rendering of light spectra

Artificial lighting is used to illuminate and render objects in an environment. Thus, one proxy for the quality of an SPD depends on how coloured objects with different spectral reflection factors $R(\lambda)$ are rendered. When using multi-channel LED luminaires, an object's saturation and hue can be affected depending on a light's emitted spectral shape. In 1974, the colour rendering index (CRI) was standardized to evaluate a light's quality for the colour appearance of coloured samples (Smet et al. 2016) using a single score. Most of the colourimetric methods for evaluating light sources apply a reference light representing the ideal rendition properties for coloured sampled with which a test light source is compared. As reference light, the CRI applies the Planckian radiator (Eq. 6) for CCTs below 5000 K and the mathematical CIE daylight model for CCTs above 5000 K (Guo and Houser 2004). In Fig. 4b, the daylight illuminants are plotted for 5500 K, 6500 K and 7500 K. According to the CIE 15:2004 (CIE 2004), daylight spectra for different CCTs can be computed using the formula

$$\begin{aligned} S(\lambda) = & S_0(\lambda) + M_1(x_D, y_D)\cdot S_1(\lambda) \\ & + M_2(x_D, y_D)\cdot S_2(\lambda) \end{aligned} \tag{9}$$

where $S_0(\lambda)$, $S_1(\lambda)$ and $S_2(\lambda)$ are pre-defined functions, which are reported in the CIE 15:2004 (CIE 2004). The parameter $M_1(x_D, y_D)$ and $M_2(x_D, y_D)$ can be computed using the CIExy-1931 chromaticity coordinates of the daylight's target CCT with

$$\begin{aligned} M_1 &= \frac{-1.3515 - 1.7703\cdot x_D + 5.9114\cdot y_D}{0.0241 + 0.2562\cdot x_D - 0.7341\cdot y_D} \\ M_2 &= \frac{0.0300 - 31.4424\cdot x_D + 30.0717\cdot y_D}{0.0241 + 0.2562\cdot x_D - 0.7341\cdot y_D} \end{aligned} \tag{10}$$

The chromaticity coordinate x_D can be calculated using the formula

$$x_D = \begin{cases} \frac{-4.6070\cdot 10^9}{(T)^3} + \frac{2.9678\cdot 10^6}{(T)^2} + \frac{0.09911\cdot 10^3\,\mathrm{K}}{(T)} + 0.244063, \\ \text{if} 4000\mathrm{K} \le T \le 7000\mathrm{K} \\ \frac{-2.0064\cdot 10^9}{(T)^3} + \frac{1.9018\cdot 10^6}{(T)^2} + \frac{0.24748\cdot 10^3\,\mathrm{K}}{(T)} + 0.237040, \\ \text{if} 7000\mathrm{K} < T \le 25000\mathrm{K} \end{cases} \tag{11}$$

where T is the target CCT of the daylight illuminant. Then, the chromaticity coordinate y_D is calculated with Eq. 12.

$$y_D(T) = -3.000\cdot x_D^2 + 2.870\cdot x_D - 0.275 \tag{12}$$

The CRI R_a method is based on the idea of computing the colour shift ΔE_i of eight Munsell colour samples $i = 1, ..., 8$ under a test light $(u_{t,i}, v_{t,i})$ and a reference light $(u_{r,i}, v_{r,i})$ with the same CCT (Soltic and Chalmers 2012). For calculating the chromaticity coordinates, the Munsell colour samples' reflected spectra from the reference and test light are used, respectively. The Euclidian distance between $(U_{*t,i}, V_{*t,i}, W_{*t,i})$ and $(U_{*r,i}, V_{*r,i}, W_{*r,i})$ is computed in the CIEU*V*W*-1960 colour space after correcting for chromatic adaptation using the Von Kries transformation (Guo and Houser 2004; Babilon 2018). Then, by using the colour differences ΔE_i, the special colour rendering index $R_i = 100 - 4.6\cdot\Delta E_i$ are calculated (Soltic and Chalmers 2012) for each of the eight Munsell colour samples $i = 1, ..., 8$. Finally, the general CRI R_a are calculated, which is defined as the arithmetic mean of the eight R_i values. The maximum CRI R_a value is 100 and indicates that, on average, no colour shift of the Munsell samples between the reference and the test light source can be perceived for the CIE standard observer (Houser et al. 2016). A CRI R_a of 80 is considered as the minimum requirement for indoor lighting (Houser et al. 2016; Stefani and Cajochen 2021). However, visual appearance experiments reveal that with a CRI R_a of 95, most observers may not perceive a colour difference between the reference and test light (Houser et al. 2016). Although the CRI R_a is widely used, the metric has several shortcomings when evaluating polychromatic LED spectra from multi-channel LED luminaires. The slight peaks by the narrowband chromatic LEDs (Houser et al. 2013; Smet et al. 2016) could lead to flawed evaluations due to the arithmetic mean of the CRI R_a and the lower number of the applied Munsell samples (Houser et al. 2016). Additionally, for large colour differences ΔE_i, the R_i value can become negative. Due to these mentioned and several other limitations of the CRI R_a (see also (Houser et al. 2016)), the CIE 224:2017 (CIE 2017)

recommends using the colour fidelity index R_f for scientific purposes.

The colour fidelity index R_f is in its intent like R_a (Royer 2021), but due to methodical updates the R_f value becomes more reliable. Firstly, for computing the R_f metric, 99 colour samples are applied instead of eight (Royer 2021), allowing for a less biased evaluation of colour rendering. Secondly, when calculating R_a, the reference is switched from the black body radiator to the daylight model at 5000 K, whereby the R_f values provides a smooth transition between 4000 K and 5000 K (Royer 2021). Thirdly, the colour shifts are computed in the CAM02-UCS colour space (Smet et al. 2016), which leverages the 10° CMFs (1964) (Babilon 2018) and is perceptually more uniform than CIEU*V*W* (Smet et al. 2016), allowing to approximate the human's colour sensation better. Therefore, it is widely recommended to apply the colour fidelity index R_f (TM-30-20) as a proxy for colour rendering, which is also in accordance with the CIE recommendation (CIE 2017).

3 Quantifying the non-visual properties of artificial light

Prior to the 21st century, the classical understanding of retinal ganglion cells was that they gather the processed signals of the photoreceptors and relay frequency-encoded action potentials via their axons to retinorecipient nuclei of the brain (Foster et al. 2020). Based on the standard model of the humans' eye, it was widely believed that the rods and cones form the only photosensitive receptors for processing visual information about brightness, contrast and colour changes in the environment (Foster 2005; Fu et al. 2005; Do and Yau 2010; Do 2019; Foster et al. 2020). Retrospectively, the discovery of an additional third class of photoreceptors in the mammalian retina was a scientific journey (Levin et al. 2011, chapter 26) that began with the pioneering work by Clyde Keeler (Keeler 1927). In his paper "Iris Movements in Blind Mice" from 1927, he used a mice strain lacking both types of photoreceptors in the outer retina and found an active pupillary light reflex, which was not expected due to the absence of functional vision (Keeler 1927; Sexton et al. 2012). Compared to wild-type mice, the pupil reflex of the blind strain had a higher response latency with a diminished peak constriction, leading to the conclusion of Clyde Keeler that there might be a pathway independent of vision (Keeler 1927) for controlling the iris muscles.

One key step in the quest for this mechanism was the discovery of a novel photosensitive opsin called melanopsin by Provencio et al., which was firstly found in the dermal melanophors of frogs (Xenopus laevis) in 1998 (Provencio et al. 1998) and two years later in the inner mammalian retina (Provencio et al. 2000, 2002). Retrograde labelling from the suprachiasmatic nucleus (SCN), the primary pacemaker of the circadian system, to the rat retina with fluorescent tracer by Gooley et al. (Gooley et al. 2001) revealed that most axon projections originate from retinal ganglion cells that express the photopigment melanopsin (Gooley et al. 2001; Fu et al. 2005). The characterised melanopsin-containing retinal ganglion cells (mRGCs) in the rat retina (by Berson et al. (Berson et al. 2002)) had dendrites that stratified largely in the off-sublamina of the inner plexiform layer and a small portion of dendrites that terminated in the on-sublamina (Berson et al. 2002). After blocking the outer photoreceptor signals, Berson et al. (Berson et al. 2002) demonstrated that these mRGCs could respond intrinsically to light with a wavelength-dependent peak sensitivity λ_{Peak} of 483 nm (Berson et al. 2002; Fu et al. 2005; Do and Yau 2010; Hatori and Panda 2010). This third class of photoreceptors in the inner retina has been termed intrinsically photosensitive ganglion cells (ipRGCs) (Berson 2003) or melanopsin containing ganglion cells (mRGCs) as they can respond to light independently of rods and cones through their photopigment melanopsin (Berson et al. 2002). About 1–2% of the rodents' retinal ganglion cells are photosensitive through melanopsin (Hattar et al. 2002; Tu et al. 2005; Berson 2007; Do and Yau 2010) which is primarily located in the cell body (soma), the dendrites and parts of the axons that stratify to the optic disc (Hattar et al. 2002; Do and Yau 2010; Hatori and Panda 2010). In the human retina, however, from approximately 1.5 million retinal ganglion cells, about 3000 express melanopsin in each eye, as reported in the review by M. Hatori & S. Panda (Hatori and Panda 2010).

Unlike the rods and cones, the photopigment melanopsin is not layered in stacked discs, leading to a lower quantum catch probability of the ipRGCs and an operating range at higher irradiance levels (Lucas 2013; Do 2019). Further, as the dendrites and axons of the ipRGCs in the retina also express melanopsin, they can integrate the environmental brightness across a broader spatial retinal area (Do 2019). A known characteristic property of the rods and cones is the adaptation to a stimulus, which lets the action potential rate decrease during prolonged light innervations (Jones et al. 1989; Burkhardt 1994; Fain et al. 2001; Stockman et al. 2006). In contrast, sustained intrinsic activation of the ipRGCs causes an approximately continuous response of frequency encoded action potentials, resulting in a larger temporal integration of light (Do and Yau 2013; Do 2019). For example, a temporally decreasing response to a sustained light stimulus could cause an increasing pupil aperture even though the light conditions have not changed (Do 2019). Thus, the ipRGCs can stabilise physiological responses across broader time intervals (Do 2019). Furthermore, the ipRGCs maintain their action potential rate response for several minutes (Do 2019) after a light stimulus

is turned off, resulting in stable innervations of non-visual functions, which Michael T. Do (Do 2019) compared to a physiological low-pass filter for light fluctuations in the environment (Wong et al. 2005; Do 2019).

3.1 An action spectrum for quantifying non-visual responses

For decades, static lighting systems in office environments were designed according to their energy efficiency, colour rendering, and the legally required illuminance (in Germany) of at least 500 lx in occupied and 300 lx in unoccupied workplaces (Tan et al. 2018). For this, the spectral composition of LED light sources was adapted to meet preferred colour quality values while reaching a high luminous efficacy of radiation (LER) for energy-saving reasons (Hye Oh et al. 2014; Zandi et al. 2021a). One straightforward strategy of saving energy is to match light spectra to the sensitivity of the achromatic luminance channel (Zandi et al. 2021a) that consists, as discussed, approximately of an additive combination of L- and M-cones. In this way, a higher perceived brightness can be achieved with the same amount of power consumption. Thus, most traditional lighting systems preferentially address the retinal cone circuitry of the visual system to effectively push the LER of a lighting system (Zandi et al. 2021a).

The discovery of the ipRGCs and their far-reaching importance for circadian responses (Pauley 2004; Cajochen et al. 2005; Vethe et al. 2021) such as human alertness (Cajochen et al. 2000), cognitive performance (Sunde et al. 2020), melatonin suppression (Rahman et al. 2019), sleep (van Lieshout-van Dal et al. 2019; Blume et al. 2019), body temperature and subjective comfort ratings (Rupp et al. 2019) has led to the understanding that lighting should no longer be evaluated solely according to visual parameters but also to their degree of influence to non-visual processes (Houser et al. 2021). Light spectra need to have a certain fraction in the short-wavelength range to trigger the ipRGCs and promote non-visual physiological responses. From a practical point of view, a spectral sensitivity function is necessary to evaluate such non-visual impacts of light stimuli. As the ipRGCs' intrinsic response to light directly correlates to melatonin suppression, steady-state pupil diameter and circadian rhythm, different physiological output measures can be assessed to characterise the non-visual pathway's action spectrum and respective peak wavelength.

In a consensus paper from (Lucas et al. 2014), a standardised ipRGC sensitivity function was proposed for evaluating light spectra by using the vitamin A1 nomogram with a λ_{Peak} or 480 nm. In 2018, the proposal was adopted in the CIE S 026/E:2018 standard (CIE 2018a) as a part of the α-opic sensitivity system (Fig. 5a). This standard, the spectral absorption function of the ipRGCs was derived by applying the visual pigment nomogram of Govardovskii et al. (Govardovskii et al. 2000) with a predefined peak wavelength λ_{Peak} of 480 nm.

The resulting standardised melanopic action spectrum $s_{mel}(\lambda)$ was further corrected with the transmittance of a standard observer's ocular media with an age of 32 years, which shifts the peak wavelength towards λ_{Peak} to 490 nm. In Fig. 5a, the photon absorption of a visual pigment A1 template by Govardovskii et al. (Govardovskii et al. 2000), which has peak wavelength of 480 nm, is corrected for pre-receptoral filtering of a 32-year-old standard observer. However, the age-related spectral sensitivity of the ipRGCs can be computed for different ages, by using the five-factor lens density model by (van de Kraats and van Norren 2007). With the method stated in the CIE S026/E:2018, the shift of the age-related peak sensitivity can be simulated, showing that between a 20-year-old and a 100-year-old observer the ipRGCs' peak sensitivity deviates by 18 nm (see Fig. 5b,c).

For example, a phosphor converted white LED spectral power distribution $E_e(\lambda)$ with a CCT of ~5500 K and a pho-

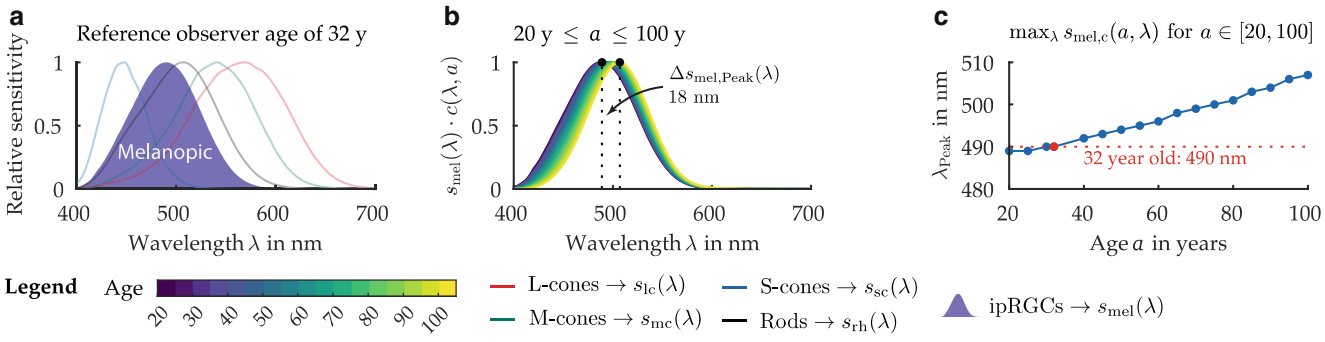

Fig. 5 Action spectrum of the ipRGCs as a function of an observer's age. (The Figure is reprinted from Zandi 2022 under CC BY-SA 4.0 license). **a** α-opic action spectra, **b** Age dependent ipRGC sensitivity, **c** Shift of ipRGC peak response

Abb. 5 Empfindlichkeitskurve der ipRGCs in Abhängigkeit vom Alter eines Beobachters. (Die Abbildung stammt aus der Arbeit von Zandi 2022, übernommen mit einer CC BY-SA 4.0 Lizenz). **a** α-opischen Gewichtungsfunktionen, **b** Spektrale Sensitivität der ipRGCs als Funktion des Alters, **c** Verschiebung der ipRGC Empfindlichkeit

topic illuminance E_v of 250 lx has a melanopic illuminance E_{mel}^{D65} of ~187 lx (see Sect. 3.2) when considering a 32-year-old standard observer. However, for a 70-year-old observer, the melanopic illuminance is reduced by ~65% to a E_{mel}^{D65} of ~121 lx, due to the age-related pre-receptoral filtering. For compensating such an affect, the photopic illuminance E_v needs to be increased from 250 to 388 lx, which would keep the non-visual responses steady across the two age groups.

Note that specifying a spectrum with CCT and Duv is not recommended for non-visual research purposes, as only a limited statement can be made about the level of melanopic excitation. Indeed, a higher CCT is associated with an increase in melanopic radiance (see Fig. 4a), but with multi-channel LED luminaires, even at a steady CCT with fixed Duv, the melanopic radiance could be tuned by up to 65% (Zandi et al. 2021a, c). Therefore, the spectra used for distinct lighting-related experiments should additionally report the α-opic values, which is a common practice for non-visual response related investigation (Spitschan et al. 2019b).

3.2 Metrics for estimating nocturnal melatonin suppression and other non-visual responses

Early after the discovery of the ipRGCs, Brainard et al. (Brainard et al. 2001) and Thapan et al. (Thapan et al. 2001) demonstrated that nocturnal melatonin suppression in humans can be affected by light. Thus, in addition to metrics related to visual perception, a new metric was needed for quantifying light-induced non-visual responses. The initially introduced non-visual related metrics focused on describing the nocturnal melatonin suppression. For this, Gall and Bieske (Gall and Bieske 2004) derived a circadian sensitivity function C(λ) using the data from Brainard (Brainard et al. 2001) and Thapan (Thapan et al. 2001), who derived the spectral sensitivity of the human's nocturnal melatonin suppression. The proposed C(λ) function has a peak sensitivity at 460 nm (Oh et al. 2015; Tian et al. 2021). In 2009, C(λ) (Gall and Bieske 2004) was incorporated into DIN V 5031-100, allowing to determine the biological effectiveness of light with the circadian action factor (CAF) a_{caf} (Eq. 14) or the circadian efficiency of radiation (CER) a_{cer} (Eq. 14).

$$a_{caf} = \frac{\int_{380\,nm}^{780\,nm} C\,(\lambda) \cdot S\,(\lambda)\,d\lambda}{\int_{380\,nm}^{780\,nm} V\,(\lambda) \cdot S\,(\lambda)\,d\lambda} \tag{13}$$

$$a_{cer} = \frac{\int_{380\,nm}^{780\,nm} C\,(\lambda) \cdot S\,(\lambda)\,d\lambda}{\int_{380\,nm}^{780\,nm} S\,(\lambda)\,d\lambda} \tag{14}$$

The introduced principle by DIN V 5031-100 involved that a light spectrum S(λ) is weighted with the sensitivity function for nocturnal melatonin suppression C(λ) and integrated across the visible spectrum range to obtain a measure of non-visual effectiveness; hence $X_{biol} = \int_{380\,nm}^{780\,nm} C\,(\lambda) \cdot S\,(\lambda)\,d\lambda$. In spectral optimisation, often, the ratio between a V(λ) weighted spectral power distribution and X_{biol} is computed to estimate the balance between the visual and non-visual excitation (Eq. 14). Furthermore, in applied office lighting, it is of interest to generate spectra with a higher amount of non-visual excitation while keeping the energy consumption low, which can be evaluated using the a_{cer} metric (Eq. 14) (Žukauskas et al. 2012; Oh et al. 2015). Mark S. Rea et al. (Rea et al. 2005, 2010, 2021a; Rea and Figueiro 2018) concluded from the ipRGCs' neurophysiological circuitry (Rea et al. 2021b) that a metric on light-induced nocturnal melatonin suppression needs to integrate the outer retinal photoreceptor's opponent input to the ipRGCs. Therefore, Rea et al. (Rea et al. 2005) proposed a novel sensitivity function based on the data of Brainard (Brainard et al. 2001) and Thapan (Thapan et al. 2001), exhibiting a sensitivity drop around 500 nm to consider the ipRGCs' opponent cone input. The metric was denoted as circadian stimulus (CS) and was updated several times (Truong et al. 2020) in 2010, 2012, 2018, 2020 and 2021 (Rea et al. 2010, 2012, 2020, 2021a; Rea and Figueiro 2018) to provide a better estimate of nocturnal melatonin suppression or to integrate additional parameters like the light's exposure time. According to the circadian stimulus' concept (version 2018) (Rea and Figueiro 2018), the amount of melatonin suppression can be computed in two steps. Firstly, the so-called circadian light CL_A needs to be calculated using the formula

$$CL_A = \begin{cases} l1548\left[\int s_{mel}\,(\lambda) \cdot E_e\,(\lambda)\,d\lambda \right. \\ \left. + \left(0.7 \cdot BY - 3.3 \cdot \left(1 - e^{\frac{-\int V'(\lambda) \cdot E_e(\lambda) d\lambda}{6.5}}\right)\right)\right], \\ \text{if} BY > 0 \\ 1548 \int s_{mel}(\lambda) \cdot E_e(\lambda) d\lambda \quad \text{if} BY \le 0 \end{cases} \tag{15}$$

where BY is defined as $\int \frac{s_{sc}(\lambda)}{mp(\lambda)} \cdot E_e\,(\lambda)\,d\lambda - 0.2616 \cdot \int \frac{V(\lambda)}{mp(\lambda)} \cdot E_e\,(\lambda)\,d\lambda$. The remaining values (Rea et al. 2021a) in Eq. 15 are defined as

- $E_e(\lambda)$= Spectral power distribution in $Wm^{-2}\,nm^{-1}$
- $mp(\lambda)$= Macular pigment transmittance,
- $s_{mel}(\lambda)$= Melanopsin sensitivity (corrected for pre-receptoral filtering),
- $s_{sc}(\lambda)$= S-cone sensitivity according to Smith and Pokorny (Smith and Pokorny 1975)
- $V(\lambda)$= Photopic luminous efficiency function and
- $V'(\lambda)$= Scotopic luminous efficiency function.

The CL_A value was normalised to the CIE standard illuminant A (see Fig. 4b), leading to a CL_A of 1000 at a photopic illuminance E_v of 1000 lx for such an illuminant (Rea

et al. 2021a). A sigmoidal function, defined as circadian stimulus, was derived by Rea et al. to predict the nocturnal melatonin suppression for one-hour light exposure (Rea et al. 2021a). The CS metric can be computed using the formula

$$CS = 0.7 - \frac{0.7}{1 + \left(\frac{CL_A}{355.7}\right)^{1.1026}} \tag{16}$$

As the CS is equivalent to the percentage of nocturnal melatonin suppression, a CS of 0.5 corresponds to a 50% reduction in melatonin after one-hour of light exposure. However, light can also positively influence task-related performance, sleepiness, heart rate, body temperature or alertness (Lucas et al. 2014; Lok et al. 2018; Prayag et al. 2019; Brown et al. 2021). Such non-visual responses can be primarily attributed to the ipRGCs, which also control the equilibrium-state pupil size. Originally, the CS was developed to quantify nocturnal melatonin suppression only; hence, it may not be appropriate to apply this metric as a proxy for other non-visual responses such as the circadian phase shift (Houser and Esposito 2021), although Rea et al. (Rea and Figueiro 2018) report that illumination (during the morning hours) with a CS score of at least 0.3 can improve sleep quality.

Per CIE S 026/E:2018 and DIN SPEC 5031-100, it is recommended to use the melanopic sensitivity function of the ipRGCs (see Sect. 3.1), which can also be combined with the other α-opic metrics (Brown et al. 2021). The proposed α-opic CIE concept provides a more general description of light-induced physiological responses (Lucas et al. 2014). The melanopic equivalent daylight illuminance E_{mel}^{D65} (melanopic EDI), derived by normalising the melanopic irradiance with the CIE standard Illuminant D65 (see Fig. 4b), is considered as an essential proxy to describe melatonin suppression, the circadian phase shift and the equilibrium-state pupil size (Zandi et al. 2020; Zandi and Khanh 2021) for longer and sustained light exposure conditions (al Enezi et al. 2011; Brown 2020; Schlangen and Price 2021; Brown et al. 2021).

$$E_{\text{mel}}^{D65} = \left(\frac{1.3262}{1000}\right)^{-1} \int_{380\,\text{nm}}^{780\,\text{nm}} s_{\text{mel}}(\lambda) \cdot E_e(\lambda)\, d\lambda \tag{17}$$

The melanopic EDI E_{mel}^{D65}, also denoted as melanopic illuminance, depends only on the ipRGCs but is in its intent comparable to the circadian light metric CL_A. Thus, the melanopic EDI can be integrated as a predictor into a sigmoidal function as well to model nocturnal melatonin suppression (Brown 2020; Brown et al. 2021; Giménez et al. 2022). A drawback in previous modelling attempts was that no distinction was made between artificially dilated and natural pupil size, as Brainard and Thapan's data were collected using artificially dilated pupils. For example, Spitschan et al. (Spitschan et al. 2019a) found no evidence for an S-cone contribution to acute melatonin suppression, which may be attributed to the experimental conditions or the subject's non-artificially dilated (natural) pupil size (Brown et al. 2021).

4 Towards intelligent lighting systems

For decades thermal radiators, such as incandescent light bulbs, were used in office, retail or home lighting, which were limited in their possibility to adjust visual properties such as the chromaticity or the spectral power distribution itself, as mostly the irradiance level (if any) could be controlled when using thermal radiators as light source. However, with the advent of LED technology in indoor lighting, it is possible to vary a light's chromaticity or irradiance in a dynamic fashion. Such LED systems can mimic the temporal behaviour of daylight (Wei et al. 2017; Cajochen et al. 2019; Eissfeldt et al. 2021) in terms of its correlated colour temperature (CCT) (Hye Oh et al. 2014) or make it possible to vary the illuminance across an entire day (Kompier et al. 2020) to provide better visual comfort and keeping the human's circadian system in synchronization (Kompier et al. 2020; Stefani et al. 2021).

Two type of LED technologies exists with which the shape of a spectral power distribution (SPD) and hence its colourimetrics may be varied. Firstly, on top of a blue LED chip a phosphor coat mixture can be added. Typically, phosphor converted white LEDs feature a peak in the short wavelength range and a wider filled spectral radiance part in the middle to long wavelength range due to the emitted light by the phosphor coat (see Fig. 2b). While in this way distinct SPD's can be reached, the SPD is static during operation in the lighting system and can no longer be changed. The second way of generating polychromatic spectra is to leverage multi-channel LED luminaires, where distinct LED colours are combined and additively mixed (Fig. 6a).

In smart lighting systems, mostly multi-channel LED luminaires are applied as they allow occupants to vary the chromaticity of the illumination or other lighting-related metrics that were discussed in Sects. 2 and 3. Thus, most connected LED lighting systems, also known as smart lighting systems, enable occupants to adjust the CCT i.e., chromaticity or irradiance of a lighting system freely or to run a pre-defined profile for automated light adjustments (Zandi et al. 2021a). However, when using smart lighting in office buildings, usually closed-loop control systems are of interest, which utilize feedback from environmental sensors (Chew et al. 2016), allowing to adapt the indoor light's irradiance or chromaticity (Tang et al. 2018) to the natu-

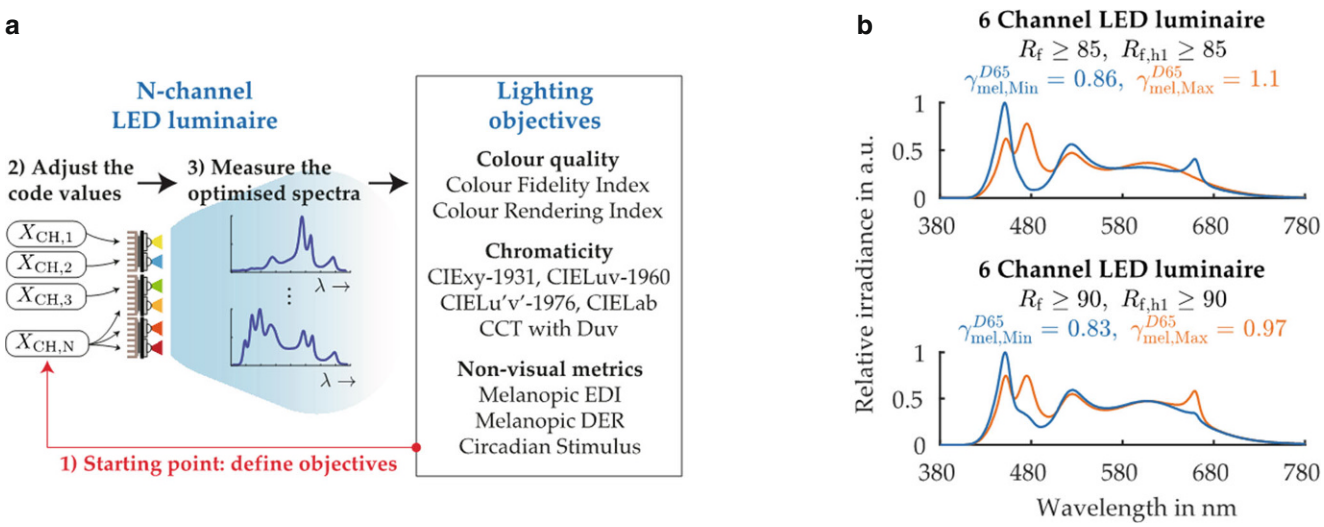

Fig. 6 When combining several LED primaries, the individual LED spectra can be additively mixed via a diffusor glass to generate polychromatic spectra that feature different lighting characteristics. The spectral shape of the polychromatic spectrum depends on the dimming level of each individual LED. One challenge when applying multi-channel LED luminaire in interior lighting is to find the best duty cycle combination of the n-channels that fulfil the desired lighting objectives, such as chromaticity, colour rendering or melanopic EDI. Usually, spectral optimization is performed for such tasks. Multi-channel LED luminaires can adjust different shapes of SPDs during operation, making them a key technology for smart lighting. (The Figure is reprinted from Zandi 2022 under CC BY-SA 4.0 license)

Abb. 6 Wenn mehrere LEDs unterschiedlicher Farben miteinander kombiniert werden, können die einzelnen LED-Spektren über einen Diffusor additiv gemischt werden, um unterschiedliche polychromatische Spektren mit definierten Charakteristiken zu erzeugen. Das polychromatische Spektrum hängt grundsätzlich von der Dimmstufe jeder einzelnen LED ab. Daher ist eine Herausforderung bei der Anwendung von Mehrkanal LED-Leuchten in der Innenraumbeleuchtung, die Kombination der Dimmstufen der *n*-Kanäle zu finden, welche das gewünschte Beleuchtungsziel, wie den Farbort, Farbwiedergabe oder melanopische Beleuchtungsstärke erfüllen. Üblicherweise werden für solche Aufgaben spektrale Optimierungsverfahren eingesetzt. Mehrkanal LED-Leuchten können verschiedene Arten von Spektren generieren, was sie zu einer Schlüsseltechnologie für die intelligente Beleuchtung macht. (Die Abbildung stammt aus der Arbeit von Zandi 2022, übernommen mit einer CC BY-SA 4.0 Lizenz)

ral daylight outside of the office or adapting the illumination to other environmental indoor conditions. For example, the light's illuminance in the indoor environment could be coupled to daylight sensors outside of the building to dim the artificial light if sufficient daylight for harvesting is available (Hughes and Dhannu 2008; Chiogna et al. 2012; Caicedo and Pandharipande 2016). Next, by using occupant sensors at workplace desks, a light's dimming level could be reduced automatically if the workplace is not occupied (Nagy et al. 2016; Caicedo and Pandharipande 2016). Such closed-loop smart lighting systems interact with integrated sensor information for efficient recourse administration, making it highly attractive to save energy costs in buildings with up to 17 to 60% (Chew et al. 2016), compared to static lighting systems.

Recent studies indicate, however, that if automated lighting systems are optimised to be energy efficient only, the visual comfort of the users could suffer as the individual user's preference regarding chromaticity and illuminance may not be acknowledged (Jennings et al. 2000; Gunay et al. 2013; Nagy et al. 2016; Cheng et al. 2016; Zandi et al. 2021a). Satisfying the individual visual preferences of users, whether in office or home lighting, is the motivation of the next generation of smart lighting systems that are intelligent in a way that recommendations can be made about a user's favourite lighting adjustments at a given time.

Such intelligent lighting systems are still in the research stage. However, it is envisaged that users are equipped with a control unit that allows to make lighting adjustments in terms of chromaticity or irradiance, while an artificially intelligent system (neural networks, reinforcement learning or similar) is used to model the user's lighting adjustment behaviour across the day (Wang and Tan 2013; Cheng et al. 2016; Kandasamy et al. 2018; Tan et al. 2018; Zandi et al. 2021a). In this way, a digital twin of an user can be derived and modelled, aiming to predict the user's favourite lighting properties. A major downside of such intelligent lighting systems is that they only consider the visual aspects of an illumination, meaning its chromaticity, colour rendering or the illuminance, as other information like the shape of the light's spectral power distribution remains invisible to humans if it does not impact the visual perception.

In other words, an intelligent lighting system, could only meet the requirements of visual preference, legal requirements and energy-efficiency but the biological effectiveness would only be addressed indirectly (Zandi et al. 2021a). For example, if a user adjusts a light's chromaticity point near the Planckian locus with a CCT around 7000 K before bed-time due the visual preference, such a light setting

would be against the recommendations of biological light as higher CCTs are more likely to have a higher spectral radiance in the short wavelength-range (Zandi et al. 2021c). Thus, such a light setting could result in a conflict between a user's visual preference and the non-visual biological recommendation, as before bedtime lower melanopic EDI is recommended.

As a solution, so-called metameric spectra could be used in intelligent lighting systems, with which the melanopic illuminance can be varied without altering the visual properties (in terms of chromaticity and (il)luminance) of the illumination (see Fig. 6b). For this, two set of spectra need to be spectrally optimised on a multi-channel LED luminaire whose chromaticity and (il)luminance do not differ but its melanopic EDI is maximally different (see also (Zandi et al. 2021c)). As the melanopic EDI can be leveraged as proxy for non-visual responses (see Sect. 3.2), melatonin suppression could be controlled in the background without impairing the visual preference of the occupants in the illuminated environment. Recently, Souman et al. (Souman et al. 2018) reported that metameric spectra with fixed CCT of 2700 K and steady photopic illuminance of 175 lx can be leveraged to vary the human's melatonin production by 50%. Further, Allen et al. (Allen et al. 2018) showed with a 5-channel LED display unit that melatonin suppression and the subjectively reported sleepiness level could be varied between two sets of metameric spectra without affecting the visual appearance of the illumination.

To showcase the possibility of metameric spectra, a spectral optimisation task was performed using a 6 channel LED luminaire with four chromatic LEDs (419 nm, 475 nm, 521 nm) and two phosphor converted white LEDs with CCTs of 4655 K and 2740 K. For this, metameric spectra with the maximum difference in melanopic LED were optimised for a CCT of 6702 K (Duv = 0.003), whereby the colour fidelity index R_f was considered to be at least 85, as recommended in the TM30-20 Annex E standard (ANSI/IES 2020). With such a condition two spectra were generated with which the melanopic EDI can be varied from 430 to 550 lx, although the photopic illuminance (500 lx) and the chromaticity ($\Delta u', \Delta v' \leq 0.001$) is fixed (see Fig. 6b, upper panel). However, when increasing the colour fidelity condition from $R_f \geq 85$ to $R_f \geq 90$, the capability of varying the melanopic EDI via metameric spectra becomes more limited as shown in the analysis by Zandi et al. (Zandi et al. 2021c) and in Fig. 6b.

The concept of metameric spectra could be applied in intelligent lighting solutions to solve the potential conflict between visual preference and non-visual needs. For this, in an intelligent lighting system, the human user needs to have a control unit available in order to adjust lighting in terms of chromaticity and (il)luminance. An artificially intelligent model learns the user's setting in the background until predictions can be made about the user's preference throughout the day. Since the model is only designed for visual parameters of light, metameric spectra can now be used to automatically adjust the melanopic illuminance in the background without interfering with the model's predictions or the user's visual preference. For example, spectra in the morning hours can be optimised to have a high melanopic EDI, while in the evening hours, metameric spectra could be used that provide a low melanopic EDI.

5 Conclusion

Based on the physiological principles of the eye, it was shown that different lighting-related metrics exist for evaluating the quality of light spectra. The essential metrics for quantifying the quality of light are chromaticity and colour rendering. However, the chromaticity can also be specified using the CCT and its respective Duv value, where the latter defines the distance to the Planckian locus. Specifying the chromaticity of a light source with CCT is common practice in light science, allowing to approximate the colour of the white point is more easily. Next, it was discussed that after discovering the ipRGCs, additional metrics were introduced that were mainly concerned with the description of the spectrally dependent nocturnal melatonin suppression or approximating the action spectrum of the ipRGCs. In this sense, a standard metric to capture the non-visual effects of light is the so-called melanopic illuminance (melanopic EDI), which was also used in this work to quantify non-visual responses of metameric light.

Multi-channel LED luminaires are being pursued more frequently in interior lighting as they allow to change the spectrum by varying the dimming levels of individual LEDs (see Fig. 6a). Thus, with such luminaires, polychromatic spectra can be generated that feature a specific chromaticity, colour rendering and melanopic EDI. Especially when applying multi-channel LED luminaires in intelligent illumination systems, it is possible that a conflict could arise when users evaluate light solely according to visual properties but unintentionally neglect the non-visual effect. Therefore, it was recommended in this work to use metameric spectra, i.e. to adjust the melanopic EDI in the background independently of the visual properties of light.

Modern working environments require that people spend most of their working time indoors, leading to insufficient daylight stimulation necessary to synchronize the human circadian rhythm. Therefore, indoor lighting has become increasingly essential to compensate for the lack of daylight and to achieve better well-being, both physiologically and psychologically. In addition to this aspect, workplace safety also plays a significant role in interior lighting since only an optimally illuminated workplace in production or an

office environment can enable excellent visual performance concerning visual acuity or human reaction time. Thus, in the future, the legal regulations of workplace lighting (minimum illuminance and preventing glare artefacts) must be considered with the new research findings on the light-induced effects on humans, which currently pursue the goal of enhancing the visual preference or maximizing the non-visual responses.

Typically, intelligent lighting systems are integrated into larger office facilities, meaning that several luminaires need to be considered when performing spectral optimization. One major disadvantage of applying metameric spectra is that they must be computed using meta-heuristic spectral optimization methods (Zandi et al. 2021a), which are computationally intensive and do not work in real-time. The scalability of these optimization methods is limited, which might affect the implementation of metameric spectra in larger office facilities. A workaround would be to derive a look-up table of metameric spectra for every chromaticity that an user could adjust on a multi-channel luminaire, which, however, would not be practical. Therefore, the key technology to realize the discussed concept of metameric spectra in intelligent illumination systems is to develop a real-time spectral optimization method that allows the computation of metameric spectra for any chromaticity. Unfortunately, such a method does not yet exist and is considered in the field of light science as the missing link before the next generation of intelligent illumination systems with which metameric spectra could be pursued.

Acknowledgements This research was funded by the Deutsche Forschungsgemeinschaft (DFG, German Research Foundation)—450636577. Section two and three of this work are reprinted from Babak Zandi's doctoral thesis, entitled "*On Modelling the Human Pupil Light Response and Developing a Deep Learning-Driven Spectral Optimisation Framework to Simulate the Metameric Limits of the Melanopic Stimulus Space*" (Technical University of Darmstadt, 2022) and the segments were not quoted.

Funding Open Access funding enabled and organized by Projekt DEAL.

References

Allen AE, Hazelhoff EM, Martial FP et al (2018) Exploiting metamerism to regulate the impact of a visual display on alertness and melatonin suppression independent of visual appearance. Sleep 41:1–7. https://doi.org/10.1093/sleep/zsy100

ANSI/IES (2020) TM-30-20: IES method for evaluating light source color rendition. New York

Babilon S (2018) On the Color Rendition of White Light Sources in Relation to Memory Preference. PhD thesis. Technical University of Darmstadt

Berson D (2003) Strange vision: ganglion cells as circadian photoreceptors. Trends Neurosci 26:314–320. https://doi.org/10.1016/S0166-2236(03)00130-9

Berson DM (2007) Phototransduction in ganglion-cell photoreceptors. Pflügers Arch Eur J Physiol 454:849–855. https://doi.org/10.1007/s00424-007-0242-2

Berson DM, Dunn FA, Takao M (2002) Phototransduction by retinal ganglion cells that set the circadian clock. Science 295(80):1070–1073. https://doi.org/10.1126/science.1067262

Blume C, Garbazza C, Spitschan M (2019) Effects of light on human circadian rhythms, sleep and mood. Somnologie 23:147–156. https://doi.org/10.1007/s11818-019-00215-x

Bodrogi P, Vinh Q, Khanh T (2019) Correlations among lighting quality metrics for interior lighting. Light Res Technol 51:1192–1207. https://doi.org/10.1177/1477153518818856

Boyce P, Smet K (2014) LRT symposium "Better metrics for better lighting"—a summary. Light Res Technol 46:619–636. https://doi.org/10.1177/1477153514558161

Brainard GC, Hanifin JP, Greeson JM et al (2001) Action spectrum for melatonin regulation in humans: evidence for a novel circadian photoreceptor. J Neurosci 21:6405–6412. https://doi.org/10.1523/JNEUROSCI.21-16-06405.2001

Brown TM (2020) Melanopic illuminance defines the magnitude of human circadian light responses under a wide range of conditions. J Pineal Res. https://doi.org/10.1111/jpi.12655

Brown TM, Thapan K, Arendt J et al (2021) S-cone contribution to the acute melatonin suppression response in humans. J Pineal Res. https://doi.org/10.1111/jpi.12719

Burkhardt D (1994) Light adaptation and photopigment bleaching in cone photoreceptors in situ in the retina of the turtle. J Neurosci 14:1091–1105. https://doi.org/10.1523/JNEUROSCI.14-03-01091.1994

Caicedo D, Pandharipande A (2016) Daylight and occupancy adaptive lighting control system: an iterative optimization approach. Light Res Technol 48:661–675. https://doi.org/10.1177/1477153515587148

Cajochen C, Zeitzer JM, Czeisler CA, Dijk D-J (2000) Dose-response relationship for light intensity and ocular and electroencephalographic correlates of human alertness. Behav Brain Res 115:75–83. https://doi.org/10.1016/S0166-4328(00)00236-9

Cajochen C, Münch M, Kobialka S et al (2005) High sensitivity of human melatonin, alertness, thermoregulation, and heart rate to short wavelength light. J Clin Endocrinol Metab 90:1311–1316. https://doi.org/10.1210/jc.2004-0957

Cajochen C, Freyburger M, Basishvili T et al (2019) Effect of daylight LED on visual comfort, melatonin, mood, waking performance and sleep. Light Res Technol 51:1044–1062. https://doi.org/10.1177/1477153519828419

Carroll J, Neitz J, Neitz M (2002) Estimates of L:M cone ratio from ERG flicker photometry and genetics. J Vis. https://doi.org/10.1167/2.8.1

Cavonius CR, Robbins DO (1973) Relationships between luminance and visual acuity in the rhesus monkey. J Physiol 232:239–246. https://doi.org/10.1113/jphysiol.1973.sp010267

Cheng Z, Zhao Q, Wang F et al (2016) Satisfaction based Q-learning for integrated lighting and blind control. Energy Build 127:43–55. https://doi.org/10.1016/j.enbuild.2016.05.067
Chew I, Kalavally V, Tan CP, Parkkinen J (2016) A spectrally tunable smart LED lighting system with closed-loop control. IEEE Sens J 16:4452–4459. https://doi.org/10.1109/JSEN.2016.2542265
Chiogna M, Mahdavi A, Albatici R, Frattari A (2012) Energy efficiency of alternative lighting control systems. Light Res Technol 44:397–415. https://doi.org/10.1177/1477153511427427
CIE (2004) CIE 15:2004 Colorimetry. Vienna
CIE (2017) CIE 224:2017 Colour fidelity index for accurate scientific use. Vienna
CIE (2018a) CIE S 026/E:2018 CIE system for metrology of optical radiation for ipRGC-influenced responses to light. Austria, Vienna https://doi.org/10.25039/S026.2018
CIE (2018b) CIE 015:2018 Colorimetry, 4th edn. Vienna
Conway BR, Chatterjee S, Field GD et al (2010) Advances in color science: from retina to behavior. J Neurosci 30:14955–14963. https://doi.org/10.1523/JNEUROSCI.4348-10.2010
Conway BR, Eskew RT, Martin PR, Stockman A (2018) A tour of contemporary color vision research. Vision Res 151:2–6. https://doi.org/10.1016/j.visres.2018.06.009
Dacey DM (2000) Parallel pathways for spectral coding in primate retina. Annu Rev Neurosci 23:743–775. https://doi.org/10.1146/annurev.neuro.23.1.743
DiLaura DL (2009) Why we need lighting quality metrics. Leukos 6:4–6. https://doi.org/10.1080/15502724.2009.10732114
Do MTH (2019) Melanopsin and the intrinsically photosensitive retinal ganglion cells: biophysics to behavior. Neuron 104:205–226. https://doi.org/10.1016/j.neuron.2019.07.016
Do MTH, Yau K-W (2010) Intrinsically photosensitive retinal ganglion cells. Physiol Rev 90:1547–1581. https://doi.org/10.1152/physrev.00013.2010
Do MTH, Yau KW (2013) Adaptation to steady light by intrinsically photosensitive retinal ganglion cells. Proc Natl Acad Sci U S A 110:7470–7475. https://doi.org/10.1073/pnas.1304039110
Durmus D (2021) Correlated color temperature: Use and limitations. Light Res Technol. https://doi.org/10.1177/14771535211034330
Eissfeldt A, Zandi B, Herzog A, Khanh TQ (2021) Quantifying observer metamerism of LED spectra which chromatically mimic natural daylight. Opt Express 29:38168. https://doi.org/10.1364/OE.433411
al Enezi J, Revell V, Brown T et al (2011) A "melanopic" spectral efficiency function predicts the sensitivity of melanopsin photoreceptors to polychromatic lights. J Biol Rhythms 26:314–323. https://doi.org/10.1177/0748730411409719
Fain GL, Matthews HR, Cornwall MC, Koutalos Y (2001) Adaptation in vertebrate photoreceptors. Physiol Rev 81:117–151. https://doi.org/10.1152/physrev.2001.81.1.117
Field GD, Gauthier JL, Sher A et al (2010) Functional connectivity in the retina at the resolution of photoreceptors. Nature 467:673–677. https://doi.org/10.1038/nature09424
Foster RG (2005) Neurobiology: bright blue times. Nature 433:698–699. https://doi.org/10.1038/433698a
Foster RG, Hughes S, Peirson SN (2020) Circadian photoentrainment in mice and humans. Biology 9:180. https://doi.org/10.3390/biology9070180
Fu Y, Liao H-W, Do MTH, Yau K-W (2005) Non-image-forming ocular photoreception in vertebrates. Curr Opin Neurobiol 15:415–422. https://doi.org/10.1016/j.conb.2005.06.011
Gall D, Bieske K (2004on) Definition and measurement of circadian radiometric quantities. In: Proceedings of the CIE symposium 2004 on light and health: non-visual effects Vienna, pp 129–132
Geerdinck LM, Van Gheluwe JR, Vissenberg MCJM (2014) Discomfort glare perception of non-uniform light sources in an office setting. J Environ Psychol 39:5–13. https://doi.org/10.1016/j.jenvp.2014.04.002
Gegenfurtner KR (2003) Cortical mechanisms of colour vision. Nat Rev Neurosci 4:563–572. https://doi.org/10.1038/nrn1138
Gegenfurtner KR, Sharpe LT (1999) Color vision: from genes to perception. Cambridge University Press, Cambridge
Giménez MC, Stefani O, Cajochen C et al (2022) Predicting melatonin suppression by light in humans: Unifying photoreceptor-based equivalent daylight illuminances, spectral composition, timing and duration of light exposure. J Pineal Res. https://doi.org/10.1111/jpi.12786
Gooley JJ, Lu J, Chou TC et al (2001) Melanopsin in cells of origin of the retinohypothalamic tract. Nat Neurosci 4:1165–1165. https://doi.org/10.1038/nn768
Gooley JJ, Lu J, Fischer D, Saper CB (2003) A broad role for Melanopsin in nonvisual photoreception. J Neurosci 23:7093–7106. https://doi.org/10.1523/JNEUROSCI.23-18-07093.2003
Govardovskii V, Fyhrquist N, Reuter T et al (2000) In search of the visual pigment template. Vis Neurosci 17:509–528. https://doi.org/10.1017/S0952523800174036
Guild J (1931) The colorimetric properties of the spectrum. Philos Trans R Soc London Ser A 230:149–187. https://doi.org/10.1098/rsta.1932.0005
Gunay HB, O'Brien W, Beausoleil-Morrison I (2013) A critical review of observation studies, modeling, and simulation of adaptive occupant behaviors in offices. Build Environ 70:31–47. https://doi.org/10.1016/j.buildenv.2013.07.020
Guo X, Houser K (2004) A review of colour rendering indices and their application to commercial light sources. Light Res Technol 36:183–197. https://doi.org/10.1191/1365782804li112oa
Hamedani Z, Solgi E, Skates H et al (2019) Visual discomfort and glare assessment in office environments: a review of light-induced physiological and perceptual responses. Build Environ 153:267–280. https://doi.org/10.1016/j.buildenv.2019.02.035
Hamedani Z, Solgi E, Hine T et al (2020a) Lighting for work: A study of the relationships among discomfort glare, physiological responses and visual performance. Build Environ 167:106478. https://doi.org/10.1016/j.buildenv.2019.106478
Hamedani Z, Solgi E, Hine T, Skates H (2020b) Revealing the relationships between luminous environment characteristics and physiological, ocular and performance measures: an experimental study. Build Environ 172:106702. https://doi.org/10.1016/j.buildenv.2020.106702
Hatori M, Panda S (2010) The emerging roles of melanopsin in behavioral adaptation to light. Trends Mol Med 16:435–446. https://doi.org/10.1016/j.molmed.2010.07.005
Hattar S, Liao H-W, Takao M et al (2002) Melanopsin-containing retinal ganglion cells: architecture, projections, and intrinsic photosensitivity. Science 295:1065–1070. https://doi.org/10.1126/science.1069609
Hering E (1920) Grundzüge der Lehre vom Lichtsinn. Springer, Berlin, Heidelberg
Hernández-Andrés J, Lee RL, Romero J (1999) Calculating correlated color temperatures across the entire gamut of daylight and skylight chromaticities. Appl Opt 38:5703. https://doi.org/10.1364/AO.38.005703
Hofer H (2005) Organization of the human trichromatic cone mosaic. J Neurosci 25:9669–9679. https://doi.org/10.1523/JNEUROSCI.2414-05.2005
Houser KW, Esposito T (2021) Human-centric lighting: foundational considerations and a five-step design process. Front Neurol. https://doi.org/10.3389/fneur.2021.630553
Houser K, Mossman M, Smet K, Whitehead L (2016) Tutorial: color rendering and its applications in lighting. LEUKOS 12:7–26. https://doi.org/10.1080/15502724.2014.989802
Houser K, Boyce P, Zeitzer J, Herf M (2021) Human-centric lighting: myth, magic or metaphor? Light Res Technol 53:97–118. https://doi.org/10.1177/1477153520958448
Houser KW, Wei M, David A et al (2013) Review of measures for light-source color rendition and considerations for a two-measure

system for characterizing color rendition. Opt Express 21:10393. https://doi.org/10.1364/OE.21.010393
Hu Y, Wei M, Luo MR (2020) Observer metamerism to display white point using different primary sets. Opt Express 28:20305. https://doi.org/10.1364/OE.395568
Hughes RF, Dhannu SS (2008) Substantial energy savings through adaptive lighting. In: 2008 IEEE Electrical Power and Energy Conference—Energy Innovation
Jennings BJ, Martinovic J (2014) Luminance and color inputs to mid-level and high-level vision. J Vis 14:9–9. https://doi.org/10.1167/14.2.9
Jennings JD, Rubinstein FM, DiBartolomeo D, Blanc SL (2000) Comparison of control options in private offices in an advanced lighting controls testbed. J Illum Eng Soc 29:39–60. https://doi.org/10.1080/00994480.2000.10748316
Johnson CA (1976) Effects of luminance and stimulus distance on accommodation and visual resolution. J Opt Soc Am 66:138. https://doi.org/10.1364/JOSA.66.000138
Jones GJ, Crouch RK, Wiggert B et al (1989) Retinoid requirements for recovery of sensitivity after visual-pigment bleaching in isolated photoreceptors. Proc Natl Acad Sci 86:9606–9610. https://doi.org/10.1073/pnas.86.23.9606
Kandasamy NK, Karunagaran G, Spanos C et al (2018) Smart lighting system using ANN-IMC for personalized lighting control and daylight harvesting. Build Environ 139:170–180. https://doi.org/10.1016/j.buildenv.2018.05.005
Keeler CE (1927) Iris movements in blinde mice. Am J Physiol Content 81:107–112. https://doi.org/10.1152/ajplegacy.1927.81.1.107
Kelly KL (1963) Lines of constant correlated color temperature based on macAdam's (u,υ) uniform chromaticity transformation of the CIE diagram. J Opt Soc Am 53:999. https://doi.org/10.1364/JOSA.53.000999
Kingdom FAA, Mullen KT (1995) Separating colour and luminance information in the visual system. Spat Vis 9:191–219. https://doi.org/10.1163/156856895X00188
Kompier ME, Smolders KCHJ, de Kort YAW (2020) A systematic literature review on the rationale for and effects of dynamic light scenarios. Build Environ 186:107326. https://doi.org/10.1016/j.buildenv.2020.107326
van de Kraats J, van Norren D (2007) Optical density of the aging human ocular media in the visible and the UV. J Opt Soc Am A 24:1842. https://doi.org/10.1364/JOSAA.24.001842
Kremers J, Scholl HPN, Knau H et al (2000) L/M cone ratios in human trichromats assessed by psychophysics, electroretinography, and retinal densitometry. J Opt Soc Am A 17:517. https://doi.org/10.1364/JOSAA.17.000517
Kruisselbrink T, Dangol R, Rosemann A (2018) Photometric measurements of lighting quality: an overview. Build Environ 138:42–52. https://doi.org/10.1016/j.buildenv.2018.04.028
Krystek M (1985) An algorithm to calculate correlated colour temperature. Color Res Appl 10:38–40. https://doi.org/10.1002/col.5080100109
Lee BB (2004) Paths to colour in the retina. Clin Exp Optom 87:239–248. https://doi.org/10.1111/j.1444-0938.2004.tb05054.x
Levin L, Nilsson S, Ver Hoeve J et al (2011) Adler's physiology of the eye, 11th edn. Elsevier
Li C, Cui G, Melgosa M et al (2016) Accurate method for computing correlated color temperature. Opt Express 24:14066. https://doi.org/10.1364/OE.24.014066
van Dal Lieshout-van E, Snaphaan L, Bongers I (2019) Biodynamic lighting effects on the sleep pattern of people with dementia. Build Environ 150:245–253. https://doi.org/10.1016/j.buildenv.2019.01.010
Lok R, Smolders KCHJ, Beersma DGM, de Kort YAW (2018) Light, alertness, and alerting effects of white light: a literature overview. J Biol Rhythms 33:589–601. https://doi.org/10.1177/0748730418796443
Lucas RJ (2013) Mammalian inner retinal photoreception. Curr Biol 23:R125–R133. https://doi.org/10.1016/j.cub.2012.12.029
Lucas RJ, Peirson SN, Berson DM et al (2014) Measuring and using light in the melanopsin age. Trends Neurosci 37:1–9. https://doi.org/10.1016/j.tins.2013.10.004
Lucas RJ, Allen AE, Milosavljevic N et al (2020) Can we see with melanopsin? Annu Rev Vis Sci 6:453–468. https://doi.org/10.1146/annurev-vision-030320-041239
MacAdam DL (1937) Projective transformations of I C I color specifications. J Opt Soc Am 27:294. https://doi.org/10.1364/JOSA.27.000294
MacAdam DL (1942) Visual sensitivities to color differences in daylight. J Opt Soc Am 32:247. https://doi.org/10.1364/JOSA.32.000247
Martinovic J (2015) Magno-, Parvo-, Koniocellular Pathways. In: Encyclopedia of Color Science and Technology. Springer, Berlin, Heidelberg, pp 1–5
McCamy CS (1992) Correlated color temperature as an explicit function of chromaticity coordinates. Color Res Appl 17:142–144. https://doi.org/10.1002/col.5080170211
Nagy Z, Yong FY, Schlueter A (2016) Occupant centered lighting control: a user study on balancing comfort, acceptance, and energy consumption. Energy Build 126:310–322. https://doi.org/10.1016/j.enbuild.2016.05.075
Oh HJ, Yang JS, Rag DY (2014) Healthy, natural, efficient and tunable lighting: four-package white LEDs for optimizing the circadian effect, color quality and vision performance. Light Sci Appl 3:e141–e141. https://doi.org/10.1038/lsa.2014.22
Oh JH, Yoo H, Park HK, Do YR (2015) Analysis of circadian properties and healthy levels of blue light from smartphones at night. Sci Rep 5:11325. https://doi.org/10.1038/srep11325
Ohno Y (2014) Practical Use and Calculation of CCT and Duv. LEUKOS 10:47–55. https://doi.org/10.1080/15502724.2014.839020
Osterhaus WKE (2005) Discomfort glare assessment and prevention for daylight applications in office environments. Sol Energy 79:140–158. https://doi.org/10.1016/j.solener.2004.11.011
Otake S, Cicerone CM (2000) L and M cone relative numerosity and red-green opponency from fovea to midperiphery in the human retina. J Opt Soc Am A 17:615. https://doi.org/10.1364/JOSAA.17.000615
Pauley SM (2004) Lighting for the human circadian clock: recent research indicates that lighting has become a public health issue. Med Hypotheses 63:588–596. https://doi.org/10.1016/j.mehy.2004.03.020
Prayag A, Münch M, Aeschbach D et al (2019) Light modulation of human clocks, wake, and sleep. Clocks Sleep 1:193–208. https://doi.org/10.3390/clockssleep1010017
Provencio I, Jiang G, De Grip WJ et al (1998) Melanopsin: an opsin in melanophores, brain, and eye. Proc Natl Acad Sci 95:340–345. https://doi.org/10.1073/pnas.95.1.340
Provencio I, Rodriguez IR, Jiang G et al (2000) A novel human Opsin in the inner retina. J Neurosci 20:600–605. https://doi.org/10.1523/JNEUROSCI.20-02-00600.2000
Provencio I, Rollag MD, Castrucci AM (2002) Photoreceptive net in the mammalian retina. Nature 415:493–493. https://doi.org/10.1038/415493a
Rahman SA, Wright KP, Lockley SW et al (2019) Characterizing the temporal dynamics of melatonin and cortisol changes in response to nocturnal light exposure. Sci Rep 9:19720. https://doi.org/10.1038/s41598-019-54806-7
Rea M, Figueiro M (2018) Light as a circadian stimulus for architectural lighting. Light Res Technol 50:497–510. https://doi.org/10.1177/1477153516682368
Rea M, Figueiro M, Bierman A, Hamner R (2012) Modelling the spectral sensitivity of the human circadian system. Light Res Technol 44:386–396. https://doi.org/10.1177/1477153511430474

Rea MS, Figueiro MG, Bullough JD, Bierman A (2005) A model of phototransduction by the human circadian system. Brain Res Rev 50:213–228. https://doi.org/10.1016/j.brainresrev.2005.07.002

Rea MS, Figueiro MG, Bierman A, Bullough JD (2010) Circadian light. J Circadian Rhythms 8:2. https://doi.org/10.1186/1740-3391-8-2

Rea MS, Nagare R, Figueiro MG (2020) Predictions of melatonin suppression during the early biological night and their implications for residential light exposures prior to sleeping. Sci Rep 10:14114. https://doi.org/10.1038/s41598-020-70619-5

Rea MS, Nagare R, Figueiro MG (2021a) Modeling circadian phototransduction: quantitative predictions of psychophysical data. Front Neurosci. https://doi.org/10.3389/fnins.2021.615322

Rea MS, Nagare R, Figueiro MG (2021b) Modeling circadian phototransduction: retinal neurophysiology and neuroanatomy. Front Neurosci. https://doi.org/10.3389/fnins.2020.615305

Ripamonti C, Woo WL, Crowther E, Stockman A (2009) The S-cone contribution to luminance depends on the M- and L-cone adaptation levels: silent surrounds? J Vis 9:10–10. https://doi.org/10.1167/9.3.10

Robertson AR (1968) Computation of correlated color temperature and distribution temperature. J Opt Soc Am 58:1528. https://doi.org/10.1364/JOSA.58.001528

Royer MP (2021) Tutorial: background and guidance for using the ANSI/IES TM-30 method for evaluating light source color rendition. LEUKOS 00:1–41. https://doi.org/10.1080/15502724.2020.1860771

Rupp AC, Ren M, Altimus CM et al (2019) Distinct ipRGC subpopulations mediate light's acute and circadian effects on body temperature and sleep. Elife. https://doi.org/10.7554/eLife.44358

Rushton WAH, Baker HD (1964) Red/green sensitivity in normal vision. Vision Res 4:75–85. https://doi.org/10.1016/0042-6989(64)90034-3

Sagawa K (2006) Toward a CIE supplementary system of photometry: brightness at any level including mesopic vision. Ophthalmic Physiol Opt 26:240–245. https://doi.org/10.1111/j.1475-1313.2006.00357.x

Schanda J (2007) Colorimetry: understanding the CIE system, 1st edn. John Wiley & Sons, Hoboken

Schanda J, Danyi M (1977) Correlated color-temperature calculations in the CIE 1976 chromaticity diagram. Color Res Appl 2:161–163. https://doi.org/10.1002/col.5080020403

Schanda J, Mészáros M, Czibula G (1978) Calculating correlated color temperature with a desktop programmable calculator. Color Res Appl 3:65–69. https://doi.org/10.1002/col.5080030204

Schlangen LJM, Price LLA (2021) The lighting environment, its metrology, and non-visual responses. Front Neurol. https://doi.org/10.3389/fneur.2021.624861

Sexton T, Buhr E, Van Gelder RN (2012) Melanopsin and mechanisms of non-visual ocular photoreception. J Biol Chem 287:1649–1656. https://doi.org/10.1074/jbc.R111.301226

Sharpe LT, Stockman A, Jagla W, Jägle H (2005) A luminous efficiency function, V *(λ), for daylight adaptation. J Vis 5:3. https://doi.org/10.1167/5.11.3

Shevell SK, Martin PR (2017) Color opponency: tutorial. J Opt Soc Am A 34:1099. https://doi.org/10.1364/JOSAA.34.001099

Shishegar N, Boubekri M, Stine-Morrow EAL, Rogers WA (2021) Tuning environmental lighting improves objective and subjective sleep quality in older adults. Build Environ 204:108096. https://doi.org/10.1016/j.buildenv.2021.108096

Smet KAG, David A, Whitehead L (2016) Why color space uniformity and sample set spectral uniformity are essential for color rendering measures. LEUKOS 12:39–50. https://doi.org/10.1080/15502724.2015.1091356

Smith VC, Pokorny J (1975) Spectral sensitivity of the foveal cone photopigments between 400 and 500 nm. Vision Res 15:161–171. https://doi.org/10.1016/0042-6989(75)90203-5

Smith VC, Pokorny J, Lee BB, Dacey DM (2008) Sequential processing in vision: the interaction of sensitivity regulation and temporal dynamics. Vision Res 48:2649–2656. https://doi.org/10.1016/j.visres.2008.05.002

Solomon SG, Lennie P (2007) The machinery of colour vision. Nat Rev Neurosci 8:276–286. https://doi.org/10.1038/nrn2094

Soltic S, Chalmers A (2012) Differential evolution for the optimisation of multi-band white LED light sources. Light Res Technol 44:224–237. https://doi.org/10.1177/1477153511409339

Souman JL, Borra T, de Goijer I et al (2018) Spectral tuning of white light allows for strong reduction in melatonin suppression without changing illumination level or color temperature. J Biol Rhythms 33:420–431. https://doi.org/10.1177/0748730418784041

Spitschan M (2019) Melanopsin contributions to non-visual and visual function. Curr Opin Behav Sci 30:67–72. https://doi.org/10.1016/j.cobeha.2019.06.004

Spitschan M, Woelders T (2018) The method of silent substitution for examining melanopsin contributions to pupil control. Front Neurol. https://doi.org/10.3389/fneur.2018.00941

Spitschan M, Lazar R, Yetik E, Cajochen C (2019a) No evidence for an S cone contribution to acute neuroendocrine and alerting responses to light. Curr Biol 29:R1297–R1298. https://doi.org/10.1016/j.cub.2019.11.031

Spitschan M, Stefani O, Blattner P et al (2019b) How to report light exposure in human chronobiology and sleep research experiments. Clocks Sleep 1:280–289. https://doi.org/10.3390/clockssleep1030024

Stefani O, Cajochen C (2021) Should we re-think regulations and standards for lighting at workplaces? A practice review on existing lighting recommendations. Front Psychiatry. https://doi.org/10.3389/fpsyt.2021.652161

Stefani O, Freyburger M, Veitz S et al (2021) Changing color and intensity of LED lighting across the day impacts on circadian melatonin rhythms and sleep in healthy men. J Pineal Res. https://doi.org/10.1111/jpi.12714

Stockman A, Sharpe LT (2000) The spectral sensitivities of the middle- and long-wavelength-sensitive cones derived from measurements in observers of known genotype. Vision Res 40:1711–1737. https://doi.org/10.1016/S0042-6989(00)00021-3

Stockman A, Sharpe LT, Fach C (1999) The spectral sensitivity of the human short-wavelength sensitive cones derived from thresholds and color matches. Vision Res 39:2901–2927. https://doi.org/10.1016/S0042-6989(98)00225-9

Stockman A, Langendorfer M, Smithson HE, Sharpe LT (2006) Human cone light adaptation: From behavioral measurements to molecular mechanisms. J Vis 6:5–5. https://doi.org/10.1167/6.11.5

Sturgis SP, Osgood DJ (1982) Effects of glare and background luminance on visual acuity and contrast sensitivity: implications for driver night vision testing. Hum Factors J Hum Factors Ergon Soc 24:347–360. https://doi.org/10.1177/001872088202400310

Sunde E, Pedersen T, Mrdalj J et al (2020) Blue-enriched white light improves performance but not subjective alertness and circadian adaptation during three consecutive simulated night shifts. Front Psychol. https://doi.org/10.3389/fpsyg.2020.02172

Tailby C, Szmajda BA, Buzás P et al (2008) Transmission of blue (S) cone signals through the primate lateral geniculate nucleus. J Physiol 586:5947–5967. https://doi.org/10.1113/jphysiol.2008.161893

Tan F, Caicedo D, Pandharipande A, Zuniga M (2018) Sensor-driven, human-in-the-loop lighting control. Light Res Technol 50:660–680. https://doi.org/10.1177/1477153517693887

Tang SJW, Kalavally V, Ng KY et al (2018) Real-time closed-loop color control of a multi-channel luminaire using sensors onboard a mobile device. IEEE Access 6:54751–54759. https://doi.org/10.1109/ACCESS.2018.2872320

Thapan K, Arendt J, Skene DJ (2001) An action spectrum for melatonin suppression: evidence for a novel non-rod, non-cone pho-

toreceptor system in humans. J Physiol 535:261–267. https://doi.org/10.1111/j.1469-7793.2001.t01-1-00261.x
Tian H, Chen T, Hu Y et al (2021) Change of circadian effect with colour temperature and eye spectral transmittance at different ages. Light Res Technol 53:41–53. https://doi.org/10.1177/1477153520923379
Tinsley JN, Molodtsov MI, Prevedel R et al (2016) Direct detection of a single photon by humans. Nat Commun 7:12172. https://doi.org/10.1038/ncomms12172
Truong W, Zandi B, Trinh VQ, Khanh TQ (2020) Circadian metric—Computation of circadian stimulus using illuminance, correlated colour temperature and colour rendering index. Build Environ 184:107146. https://doi.org/10.1016/j.buildenv.2020.107146
Tsujimura S, Shioiri S, Nuruki A (2007) Two distinct cone-opponent processes in the L+M luminance pathway. Vision Res 47:1839–1854. https://doi.org/10.1016/j.visres.2007.03.016
Tu DC, Zhang D, Demas J et al (2005) Physiologic diversity and development of intrinsically photosensitive retinal ganglion cells. Neuron 48:987–999. https://doi.org/10.1016/j.neuron.2005.09.031
Valberg A (2005) Light vision color. Wiley
Van Den Wymelenberg K, Inanici M (2014) A critical investigation of common lighting design metrics for predicting human visual comfort in offices with daylight. LEUKOS 10:145–164. https://doi.org/10.1080/15502724.2014.881720
Vethe D, Scott J, Engstrøm M et al (2021) The evening light environment in hospitals can be designed to produce less disruptive effects on the circadian system and improve sleep. Sleep 44:1–12. https://doi.org/10.1093/sleep/zsaa194
Wang Z, Tan YK (2013) Illumination control of LED systems based on neural network model and energy optimization algorithm. Energy Build 62:514–521. https://doi.org/10.1016/j.enbuild.2013.03.029
Wei M, Yang B, Lin Y (2017) Optimization of a spectrally tunable LED daylight simulator. Color Res Appl 42:419–423. https://doi.org/10.1002/col.22094
Wong KY, Dunn FA, Berson DM (2005) Photoreceptor adaptation in intrinsically photosensitive retinal ganglion cells. Neuron 48:1001–1010. https://doi.org/10.1016/j.neuron.2005.11.016
Wool LE, Packer OS, Zaidi Q, Dacey DM (2019) Connectomic identification and three-dimensional color tuning of S-OFF midget ganglion cells in the primate retina. J Neurosci 39:7893–7909. https://doi.org/10.1523/JNEUROSCI.0778-19.2019
Wright WD (1929) A re-determination of the trichromatic coefficients of the spectral colours. Trans Opt Soc 30:141–164. https://doi.org/10.1088/1475-4878/30/4/301
Xingzhong Q (1987) Formulas for computing correlated color temperature. Color Res Appl 12:285–287. https://doi.org/10.1002/col.5080120511
Yoshi O, Blattner P (2014) Chromaticity Difference Specification for Light Sources. CIE TN 001:2014. Vienna, Austria
Zandi B (2022) On modelling the human pupil light response and developing a deep learning-driven spectral optimisation framework to simulate the metameric limits of the Melanopic stimulus space. Technical University of Darmstadt
Zandi B, Khanh TQ (2021) Deep learning-based pupil model predicts time and spectral dependent light responses. Sci Rep 11:841. https://doi.org/10.1038/s41598-020-79908-5
Zandi B, Klabes J, Khanh TQ (2020) Prediction accuracy of L- and M-cone based human pupil light models. Sci Rep 10:10988. https://doi.org/10.1038/s41598-020-67593-3
Zandi B, Eissfeldt A, Herzog A, Khanh TQ (2021a) Melanopic limits of metamer spectral optimisation in multi-channel smart lighting systems. Energies 14:527. https://doi.org/10.3390/en14030527
Zandi B, Lode M, Herzog A et al (2021b) PupilEXT: flexible open-source platform for high-resolution pupillometry in vision research. Front Neurosci. https://doi.org/10.3389/fnins.2021.676220
Zandi B, Stefani O, Herzog A et al (2021c) Optimising metameric spectra for integrative lighting to modulate the circadian system without affecting visual appearance. Sci Rep 11:23188. https://doi.org/10.1038/s41598-021-02136-y
Zhang F (2019) High-accuracy method for calculating correlated color temperature with a lookup table based on golden section search. Optik 193:163018. https://doi.org/10.1016/j.ijleo.2019.163018
Žukauskas A, Vaicekauskas R, Vitta P (2012) Optimization of solid-state lamps for photobiologically friendly mesopic lighting. Appl Opt 51:8423. https://doi.org/10.1364/AO.51.008423